Bringing back the Binnensingel

Quantifying the reductions in pluvial flooding and groundwater fluctuations from adding open water to a dense urban polder area

S.P.M. Gabriëls

UNIVERSITY
OF TWENTE.

Nelen &
Schuurmans

Master thesis

Bringing back the Binnensingel

Quantifying the reductions in pluvial flooding and groundwater fluctuations from adding open water to a dense urban polder area

Author
S.P.M. (Sjoerd) Gabriëls

Institution
University of Twente

Date
March 6, 2025

Version
Final

Supervisors

Dr. ir. M.J. (Martijn) Booij	Head supervisor	University of Twente
Dr. ir. A. (Anouk) Bomers	Daily supervisor	University of Twente
Ir. R. (Ria) Löschner-Wolleswinkel	Supervisor	Nelen & Schuurmans
MRM. M.J.J. (Menno) Blom	Daily supervisor	Nelen & Schuurmans

Preface

Already early in my studies I came to like modelling and programming. During the later years, I developed an interest in urban water management as an essential link in increasing the climate resilience of our society. I am therefore happy to present my master thesis on a research that has combined all of these interests.

I have conducted this research during a very difficult period in my life. Although it has not been easy, my thesis has served as a lifeline for me for over almost a year. Consequently, I am very grateful to have been given the opportunity by Nelen & Schuurmans and the University of Twente to execute this research with all the time and flexibility that I needed.

Specifically, I want to thank Menno Blom, who jumped in as my daily supervisor a few months into my research and always had time to spar, to tackle some questions or provide me with feedback, and most importantly, who managed to make me feel appreciated and motivated by an endless amount of enthusiasm. I want to thank Ria Löschner, whose vision, experience and clear feedback kept the research on course when I dared to start drifting afloat. I want to thank Bas van Haaren for his shaping guidance and patience during the first few months of my research. And of course, I want to thank all colleagues from Nelen & Schuurmans for helping me out throughout the research and for keeping up with my horrendous ping-pong skills.

From the university, I want to thank Anouk Bomers and Martijn Booij, who provided me with a great amount of knowledge and feedback throughout the entire process. I seldomly left with more worries than I came in with and very much enjoyed our meetings in Martijns office.

And last, but not least, I want to thank my family and friends for their ongoing support. Thank you all for the many good moments we have shared together.

I have learned a great deal while writing this thesis and hope you will do so too while reading it. Enjoy the read!

Sjoerd Gabriëls

Utrecht, March 2025

Summary

Around the world, many large cities are located in low-lying areas on soils susceptible to subsidence. This leads to a dilemma for water managers, who have to pump away water to prevent flooding without pumping away too much water, as this accelerates subsidence. Simultaneously, cities are trying to increase the robustness of their water system as a way to adapt to increasing intensities in rain and drought as a consequence of climate change. The addition of surface water is a possible measure to achieve this when groundwater levels are high, but many effects of this measure have not yet been quantified. This thesis sheds light on this measure by studying the effects of restoring the Binnensingel canal in the Dutch city of Vlaardingen on pluvial flooding and groundwater fluctuations.

To achieve this, the integral hydrodynamic model 3Di is used. Firstly, an existing schematisation is updated and the model is calibrated. Secondly, the effects of a composite rainfall event with a return time of two years for a climate scenario for 2050 on the existing study area are investigated. Thirdly, the canal is implemented into the model with several variations in length, water level and connected area.

The groundwater part of the model is calibrated by tuning the infiltration, porosity and hydraulic conductivity as these were found to be the most influential in a sensitivity analysis. After calibration, the accuracy of the groundwater model is quantified and deemed to be sufficient with a mean absolute error of 0.04 m. The accuracy of the surface and sewerage part of the model is not quantifiable due to errors in historic measurements, but is qualitatively found to be sufficient.

The results show that the future rainfall event causes heavy pluvial flooding in the current situation, leading to a maximum of 25-30 cm of standing water for a duration of more than two hours and 948 vulnerable buildings throughout the study area. Implementation of the canal reduces this only slightly; by up to 2 cm in depth, 15 minutes in duration and 19 vulnerable buildings. Groundwater fluctuations have a magnitude of up to 30 cm in the current situation and are reduced only locally around the Binnensingel when a canal is added. Variants of the canal with a higher connected area and a lower water level are found to be the most effective.

Future research can benefit from the usage of a wider range of rainfall events that are run in series alternated with dry events. This will give more insight in the long-term groundwater fluctuations and the effect of a canal during less intense, yet more frequent rainfall events.

Samenvatting

Veel grote steden liggen wereldwijd in laaggelegen gebieden op gronden gevoelig voor verzakking. Dit veroorzaakt een dillemma voor watermanagers, die water moeten wegpompen om wateroverlast te voorkomen zonder zoveel water weg te pompen dat het de verzakking versnelt. Tegelijkertijd willen de steden met het oog op intensere regenval én droogte door klimaatverandering hun watersysteem robuuster maken. Het toevoegen van open water is een mogelijke manier om dit te bereiken als de grondwaterstanden hoog zijn, maar veel effecten hiervan zijn nog niet gekwantificeerd. Deze studie gaat hierop in door de effecten van het terugbrengen van de gracht op de Binnensingel in Vlaardingen op wateroverlast en grondwaterfluctuaties te onderzoeken.

Hiervoor wordt het integraal hydrodynamisch model 3Di gebruikt. Eerst wordt een bestaande schematisatie geüpdated en het model gekalibreerd. Daarna worden de effecten van een compositietbui met een herhalingstijd van 2 jaar voor het klimaat van 2050 op het huidige studiegebied bepaald. Tot slot wordt de gracht aan het model toegevoegd met varianten in lengte, waterniveau en aangesloten oppervlak.

Het grondwaterdeel van het model is gekalibreerd op de parameters voor infiltratie, porositeit en doorlatendheid nadat deze in een gevoeligheidsanalyse het meest invloedrijk zijn gebleken. Na de kalibratie is de nauwkeurigheid van het grondwatermodel voldoende bevonden met een gemiddelde absolute fout van 0.04 m. De accuraatheid van het oppervlakte- en riooldeel van het model is niet te kwantificeren door meetfouten in de historische metingen, maar is kwalitief voldoende gebleken.

De resultaten laten zien dat de toekomstige bui hevige wateroverlast in de huidige situatie veroorzaakt: water-op-straat heeft een maximale diepte van 25-30 cm en duur van meer dan twee uur en leidt tot 948 kwetsbare panden in het hele studiegebied. Het toevoegen van de gracht vermindert dit slechts met maximaal 2 cm in diepte, 15 minuten in duur en 19 kwetsbare panden. Grondwaterfluctuatie heeft in de huidige situatie een grootte van 30 cm en wordt bij het toevoegen van de gracht alleen lokaal rondom de Binneningel verkleind. De varianten van de gracht met een hoog aangesloten oppervlak of een laag waterpeil zijn het meest effectief.

Verder onderzoek zou baat hebben bij het doorrekenen van meerdere buien die in serie met periodes van droogte worden gedraaid. Dit zal meer inzicht geven in de grondwaterfluctuaties op lange termijn en het effect van de gracht gedurende minder intense, maar vaker voorkomende buien.

Contents

1 Introduction

1.1 Context

Many of the world's cities are located in lowland coastal areas, which makes millions of people vulnerable to flooding (McGranahan et al., 2007; Neumann et al., 2015). The challenges this induces are amplified by the fact that the soil in coastal areas typically consists of mostly clay and peat, both of which are susceptible to subsidence (e.g. Brown & Nicholls, 2015; Kim et al., 2015; Stoorvogel et al., 2016). Water managers are therefore walking a fine line between not pumping away enough water, which enlarges the risk of flooding, and pumping too much, which accelerates the settling of the soil, which in turn leads to repetition of the dilemma (Gorelick & Zheng, 2015).

Climate change is contributing to this dilemma by introducing longer periods of increasingly intense periods of rain on the one hand and increasingly intense drought on the other (IPCC, 2023). Already visible in the present day, these effects of climate change are projected to get stronger, although the magnitude of change differs per location. For the Netherlands for example, the Royal Dutch Meteorological Institute (KNMI) has predicted an increase in rainfall of 4 to 7% during winter and a decrease in rainfall of -13 to -5% during summer for 2050. At the same time, rainfall during summer will become more intense: the annual maximum amount of rain in one hour is expected to increase from the current 16 mm to 27 mm around 2050 (KNMI, 2023).

For cities especially, maintaining a robust water balance will be increasingly harder. While some cities are rapidly adapting to climate change, cities in coastal lowlands often struggle with high groundwater tables (van Dorland et al., 2024; K. Wang et al., 2021). This limits the possibilities for implementation of widely-used climate adaptation measures such as retention ponds, infiltration crates and disconnecting of streets and roofs (Carmen et al., 2016; RIONED, 2014).

One of the possible measures which has sparked interest over the recent years is the paradoxical intervention of adding surface water. In theory, new surface water bodies will increase the water storage possibilities, decrease the pressure on the sewerage system and act as a stabilizer for the groundwater level. The extent of this has however not yet been researched in an integral approach, in which surface, sewerage and groundwater are combined. This study therefore focusses on quantifying the effects of the addition of surface water bodies as a

climate adaptation measure in cities susceptible to subsidence. It will do so by evaluating the effect of reinstating the canal on the Binnensingel in the Dutch city of Vlaardingen (see Section 2.1) on pluvial flooding and groundwater fluctuations using an integral hydrodynamic model.

1.2 State-of-the-art

Canals in urban areas can serve a plethora of purposes, for example retaining and storing rainwater, increasing the infiltration of rainwater into the soil, enhancing the cities aesthetic and increasing the recreational value of public spaces, improving local water quality and providing a cooling effect to its surroundings (STOWA, 2009; VMM, 1996). With the increasing focus on climate change (IPCC, 2023), most research regarding canals in cities has been done on the latter. Most researchers have found that canals can succesfully reduce the Urban Heat Island (UHI) effect (e.g. Jandaghian & Colombo, 2024; Merga et al., 2024; Y. Wang et al., 2016), although the extent varies from case to case: in some situations, open water can even increase the UHI (Steeneveld et al., 2014). On the topic of urban water quality, most research goes into water quality measuring frameworks (e.g. Sajib et al., 2024; Zhan et al., 2022), which is used by mostly governing parties to assess the quality of surface waters such as canals. For the Netherlands, these studies consistently identify sewage overflows, faulty sewer connections and contaminated surface runoff as the main risks for urban water quality (e.g. NIOO-KNAW, 2022; Schets et al., 2008). Despite the clear interest in the urban water system, no scientific sources that studied the effects of urban canals as a climate adaptation measure to decrease (ground)water hindrance or even flooding were found.

However, other climate adaptation measures regarding water management have been intensively studied and found to be effective (e.g. Fletcher, 2009; Imran et al., 2013; STOWA, 2019a). As such, measures like wadis, green roofs and infiltration crates have become common in newly built neighbourhoods (e.g. Ariza et al., 2019; Eigenhuijsen et al., 2009; Melville-Shreeve et al., 2017) and are increasingly implemented into city redevelopment projects as municipalities realise the importance of an integrated approach to urban water management (de Jong et al., 2001). Still, the majority of this research has been done with case studies of cities with highly permeable soils or deeper groundwater levels (e.g. RIONED, 2014; Steenbergen, 2008; Wiebing, 2023), while studies have pointed out that popular infiltration-oriented measures are rarely successful in areas with higher groundwater levels (de Jong et al., 2001).

Traditionally, these studies have been experimental and were often done without storm conditions. With increasing computational power and more detailed modelling software, integral approaches in which climate adaptation measures are included in hydrodynamic or hydrological models of cities have become popular. Examples of these modelling softwares are HEC-RAS, Infoworks ICM, 3Di, D-Hydro and Tygron. In general however, the choice of software is of little importance on the accuracy of the model, which is influenced more by the quality of input data and skills of the modeller (Gan et al., 1997; STOWA, 2017) and the applicability of the software to a specific case. Nevertheless, a modelling software which has the ability to couple 1D models (for sewerage systems) and 2D models (for surface flows) can yield more accurate results than a separate 1D or 2D model (e.g. Guo et al., 2021; Patra et al., 2016; Vozinaki et al., 2017) and is thus preferable in an urban setting.

1.3 Research gap

A lot of research on climate adaptation focusses on infiltration possibilities, which means that many results from these studies are not applicable to areas in which infiltration possibilities are naturally low due to high groundwater levels and/or subsidence. In these areas, stabilizing the groundwater level is of higher importance than increasing infiltration. Although it is known that adding urban canals is a possible method to stabilize groundwater levels, research on urban open water mostly focusses on water quality and cooling effects. Quantitative integral research into the effects urban open water has on reducing pluvial flooding and fluctuations of the groundwater level is still missing.

1.4 Aim and research questions

The aim of the study is to quantify the effect of adding surface water as a climate adaptation measure on pluvial flooding and groundwater fluctuations. This will be done on neighbourhood level for a city in the western part of the Netherlands. (see Sections 1.5 and 2.1).

An up-to-date 3Di-model of the study area, containing the schematisation of the surface, waterways, buildings and sewerage system, is provided by Nelen & Schuurmans. In order to effectively asses groundwater fluctuations, groundwater flow will be added to this schematisation. The model will therefore be calibrated and subsequently validated, until its outputs sufficiently resemble historic measurements. This leads to the first research question:

RQ1: Which model configuration and parametrization results in an acceptable simulation of reality?

The calibrated and validated model will be used to predict the effects of future rainfall. A future design rainfall event will be selected and applied to the model, after which the results can be determined in terms of depth and duration of pluvial flooding and fluctuations of the groundwater level.

RQ2: What are the effects on pluvial flooding and groundwater fluctuations when a future rainfall event is applied on an urban area with high groundwater levels?

Increasing the amount of surface water hypothetically decreases pluvial flooding and has a stabilising effect on the groundwater table. To assess this hypothesis and quantify the expected effects, various variants of a canal will be added to the schematisation of the study area. To make maximum use of this measure, parts of the study area will be disconnected from the combined sewerage system and connected to the added canal. The same future rainfall event as used for RQ2 will be applied to the altered model and pluvial flooding and groundwater fluctuations are determined once again. Comparing these results with those from RQ2 leads to answer the third research question:

RQ3: What is the influence of the addition of a canal on pluvial flooding and groundwater fluctuations in an urban area with high groundwater levels?

1.5 Scope

The study includes 2D surface and groundwater flow in combination with 1D sewerage flow. This includes hydrological processes such as infiltration. Groundwater flow below the phreatic aquifer is excluded from the study, as the time scales of these flows exceed the simulation length used in this study and are therefore expected to have a very small influence. Evaporation, heat stress, wind effects and water quality are excluded from the study as well.

The study is limited to future climate conditions for approximately 2050, as this ensures applicability of the results beyond the current climate conditions, without being too susceptible to variety in climate models. Additionally, the KNMI has predicted values for meteorologic changes around 2050 and design rainfall events based on these values have been derived (RIONED, 2020; STOWA, 2019b).

As a case for the study, the Oostwijk area in the Dutch city of Vlaardingen will be used. The Oostwijk is one of the oldest neighbourhoods of Vlaardingen and is with its dense housing and large area of impervious surfaces exemplary for many neighbourhoods in Dutch cities. Additionally, the Oostwijk has known problems with subsidence in the past, which has lead to the groundwater level being close to the surface. The combination of a high amount of impervious area with high groundwater levels makes that the Oostwijk is highly susceptible to pluvial flooding.

1.6 Report outline

This chapter has given an introduction to the study itself. In Chapter 2, an elaboration on the study area is given, followed by an introduction of the 3Di modelling software and a list of data sources used in the study. Chapter 3 covers the methods to answer the research questions. In chapter 4, the results of the study are presented and interpreted. Chapter 5 offers a discussion of the influence of the used methods on the results and how the results could potentially be generalized. Finally, chapter 6 states the conclusions of the study and gives recommendations for practical use of the study, as well as recommendations for future research.

2 Materials

2.1 Study area

The study area is the Oostwijk neighbourhood in the city of Vlaardingen. Vlaardingen is located in the west of the Netherlands, between the coast and the city of Rotterdam, and on the northern bank of the Nieuwe Maas river (see Figure 1a). The Oostwijk is located in the southeast of Vlaardingen. As one of the oldest neighbourhoods of the city, the Oostwijk is characterised by the relatively dense housing, a high percentage of paved area and little space for vegetation. The Oostwijk has approximately 7400 residents (CBS, 2024). The following sections elaborate on the study area in detail. A graphical overview is given in Figure 1.

2.1.1 Geography and surface water

Geographically, the Oostwijk is bound by the Oude Haven in the west, an access road in the north and east and rail tracks in the south. Surface level is located at approximately 0 m with regards to NAP (Normaal Amsterdams Peil, *Amsterdam Ordnance Datum*), with the surface elevation decreasing gradually from north to south. In the south of the study area, several streets have subsided by 30-40 cm compared to the edges of the study area. The heaviest subsidence is found in the Willem Barendszoonstraat (see Figure 1b), which at its lowest point lies 80 cm beneath the surrounding streets.

Two major roads traverse the area: the Schiedamseweg from east to west and the Binnensingel from north to south. These roads cross eachother at a large roundabout in the center. The area south of the Schiedamseweg is almost exclusively residential, with the exception of the Spoorsingel, a pond next to the eponymous street. In the absolute northwest corner of the Oostwijk, a recently added neighbourhood can be found. The remainder of the Oostwijk is a municipal park (the Oranjepark), with a few ditches in the south and a larger water feature in the north, as well as several elongated ponds along the north and east boundaries of the area.

The surface waters in the Oostwijk are divided into three different fixed water level areas, which are defined by the waterboard of Delfland (see Figure 1c). A system of weirs and culverts in between water bodies regulates the water levels. In the east of the study area an overflow is present, which discharges excess water out of the study area. The Spoorsingel in the south is a separated system, as it is fed by an overflow from the Oude Haven and drained by a small pump which pumps the water back into the Oude Haven.

2.1.2 Groundwater

Although groundwater levels in urban areas generally show large spatial variation, the average groundwater level in the Oostwijk hovers around -0.3 m NAP. Considering the surface elevation being around NAP, groundwater levels are close to the surface. In the northeast of the Oostwijk, groundwater levels are generally lower (between -0.8 and -1.0 m NAP). However, groundwater levels are lowered significantly at several locations due to leaking sewerage acting as drainage. At the Willem Barendszoonstraat, groundwater is permanently drained by a dedicated pump to prevent groundwater hindrance.

2.1.3 Sewerage system

Two different sewerages are present in the Oostwijk (see Figure 1d). The neighbourhood in the northwest of the Oostwijk has an improved separated system. The rainwater sewers of this system have one outlet in the west (to the Oude Haven) and two in the east (to the Oranjepark) and are drowned as they are located below the water level of the Oude Haven. An internal weir prevents a direct connection between the Oude Haven and the park. This makes that the first flush is directed towards the Oude Haven and only when the water pressure exceeds the crest level of the weir, excess rainwater is directed to the park. The wastewater sewers end in a pumping station from where all sewage is pumped out of the study area.

The remainder of the Oostwijk has a gravity flow combined sewerage system, which culminates at a pumping station near the Boslaan, from where all sewage water is pumped out of the study area. For severe rainfall cases, the pumping station has an spillway pump to the Nieuwe Maas. The sewerage system itself has overflows at two locations: Hofsingel and Parkweg, from where water flows into the ponds in the Oranjepark. In 2018, the entire sewage system of the Oostwijk has been inspected with cameras, which has shown that several sewers are damaged and therefore likely to be leaking. All damaged pipes are located in the south of the area.

(a) Location of the Oostwijk in the Netherlands
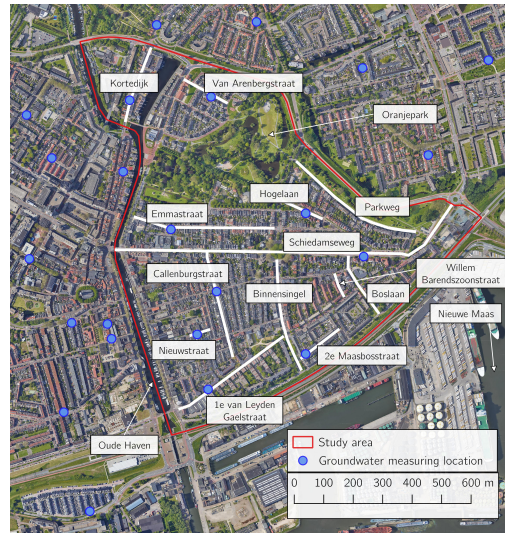
(b) Overview of relevant locations in and surrounding the Oostwijk.

(c) Overview of the surface (water) system in the Oostwijk.

(d) Overview of the sewerage system in the Oostwijk.

Figure 1: Visualisation of the Oostwijk.

2.2   3Di model

3Di is a cloud-based state-of-the-art hydrodynamic software developed by a consortium of Deltares, Delft University of Technology and Nelen & Schuurmans (3di-watermanagement.com, 2024). By applying the subgrid technique (see Section 2.2.1), 3Di can make calculations at a higher spatial resolution than conventional models, while keeping similar computation times. 3Di models can incorporate 0D, 1D and 2D surface and groundwater flows in all combinations, together with water quality, structure control and vegetation, which makes it applicable for a wide range of cases.

The following sections explain the main concepts and relevant processes used in 3Di.

2.2.1   Geography and surface water (2D)

2D computational grid

The 2D-domain in 3Di is discretised by a structured and staggered grid, in which water levels (pressures) and volumes are calculated at the centres and velocities and discharges are calculated at the edges of the computational cells (see Figure 2). Cells can be connected both horizontally, which is standard practice, and vertically, which is used for interaction between the surface and groundwater flow (see Section 2.2.2). Flow is calculated by solving the conservation of mass and momentum equation for each grid cell at each time step. To limit the resulting computational costs, quad-tree grid refinement is available (see Figure 2). This allows for multiple computational cell sizes in one grid depending on the required level of accuracy.

2D subgrid

The main influence on flow is the bathymetry or surface elevation. One would therefore prefer to calculate with the most detailed bathymetry available. This does however come with the disadvantage of strongly increasing computational times. In 3Di, the balance between computational time and accuracy is found by using the subgrid-method (Volp et al., 2013). In this method, a subgrid with a higher resolution than that of the computational grid is introduced next to the computational grid itself. Detailed input data is defined on the subgrid, while calculations are done using the computational grid. This results in a computational cell having one water level, yet different water depths inside of it. The main assumption in this process is that water levels vary less over distance than the surface elevation does, as water tends to diffuse until it is level.
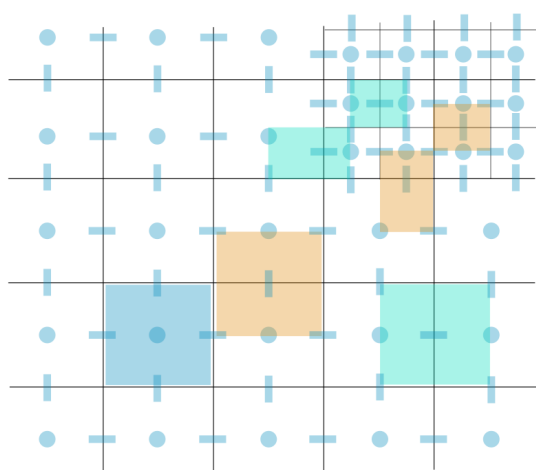
Figure 2: Example of a 2D computational grid. In the top right corner, a grid refinement is visible. The blue areas indicate the domains over which water levels are calculated. The orange and green areas indicate the domains over which discharges and velocities are calculated (Nelen & Schuurmans, 2024b).
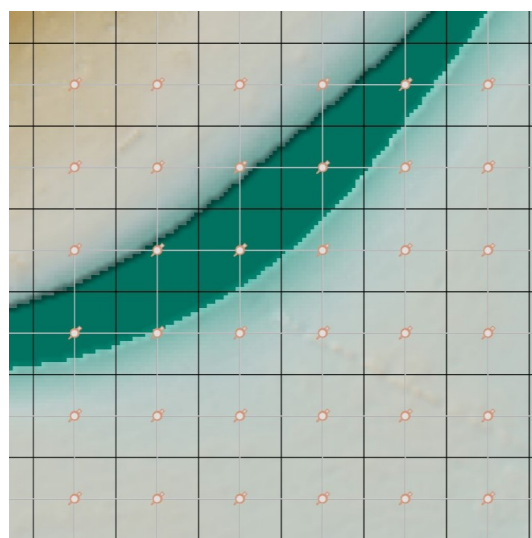
Figure 3: Example of a computational grid in combination with a higher-resolution subgrid from the 3Di-model of the Oostwijk. The black lines are the edges of the computational cells, with the white dots being the cell centers of the surface computational grid and the brown dots the cell centers of the groundwater computational grid. The colours behind indicate surface elevation as schematised on the subgrid, which is visible as the pixelated edge.

2.2.2 Groundwater (2D)

The computational grid of the groundwater domain is a copy of the 2D computational grid for surface water flow. These two grids are connected vertically, which allows for simulation of infiltration and exfiltration. The infiltration process is parametrized by the Horton Infiltration Model, which assumes an exponential decline from an initial to an equilibrium infiltration value (Horton, 1933). The exfiltration process starts when the groundwater level in a computation groundwater cell reaches the lowest bed level in the computational surface water cell above it. Additional water then is added to the surface level, while the groundwater level is virtually set equal to the surface water level to still account for the correct water pressures.

The groundwater table is assumed to be equal to the phreatic surface, so the soil above the groundwater table is assumed to be completely dry, while the soil below is fully saturated. The available groundwater storage can be defined by setting the porosity of the modelled soil. The groundwater flow is described by the Darcy equations, so the flow can be influenced by setting the hydraulic conductivity parameter (Nelen & Schuurmans, 2024a). In the saturated zone, the Dupuit condition is applied, so the flow is assumed to be fully horizontal (Dupuit, 1863).

3Di only takes the first aquifer into account. The bottom boundary of this is set to be the level of the impervious layer. Influences of groundwater bodies below this level can be incorporated into the model by the source/sink term *leakage*, which is applied on the bottom boundary.

2.2.3   Sewerage system (1D)

The 1D computational grid is, like a sewerage system, a system of lines (pipes) and nodes (manholes). Just like its 2D counterpart, the 1D computational grid is a staggered grid, where the water volumes are calculated at calculation nodes, while velocities and discharges are calculated at the centers of the flowlines between two calculation nodes (see Figure 4). Once again, the flow is calculated by solving the conservation laws of mass and momentum at each time step. The 1D computational grid is connected to the 2D computational grids by connections of the 1D nodes with the closest 2D computational grid cell centre. This allows for exchanges between the 1D and 2D domains.
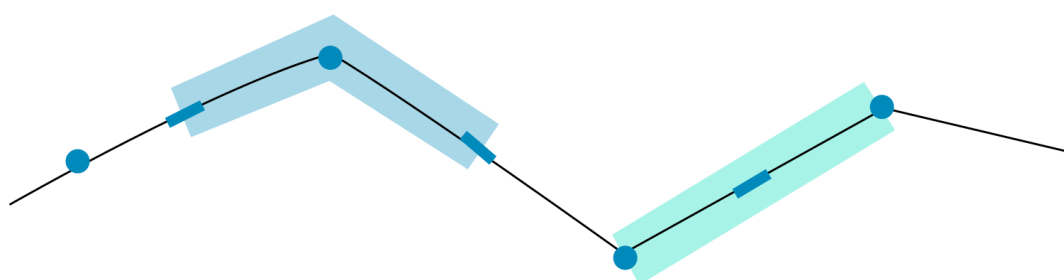
Figure 4: Example of a 1D computational grid. The blue area indicates the domain over which water levels are calculated. The green area indicates the domain over which discharges and velocities are calculated (Nelen & Schuurmans, 2024b).

2.3 Available data

Surface water levels are available via the water board of Delfland (Hoogheemraad-schap van Delfland, 2024). Groundwater levels are available as hourly measurements at nine locations throughout the study area via the online portal of the measurement sensor provider (Munisense, 2024). These measurements date back to 2019 and have been manually validated approximately once a year. Water levels in the sewerage system are measured every minute at the Callenburgstraat and at the overflow near the Parkweg and every five minutes at the pumping station Boslaan. Measurements since 2022 are provided by the municipality, together with daily cumulative running times of the individual pumps at the pumping station Boslaan. The accuracy of the sensors in the sewerage system has however not been tested since their implementation in 2015. Results of the sewerage system inspection from 2018 have also been provided by the municipality of Vlaardingen.

Precipitation data is available via three sources: the Nationale Regenradar (NRR, *National Rain Radar*), the KNMI and local measurements attached to the measurements of water levels in the sewers. Data from the NRR has been validated and is available in five minute intervals and will due to the reliability and local availability be the primary source in this study. When necessary, data from the KNMI measurement station in Rotterdam will be used, which has been validated and is available in one hour intervals, as well as the local data, which has not been validated and is available in five minute intervals.

3 Methods

3.1 Model set-up

3.1.1 Geography and surface water (2D)

In this study, no grid refinement is used due to the relatively small size of the study area and the high required accuracy. The chosen grid cell size is 10 meters.

The elevation level is given on the subgrid by a digital elevation model (DEM). Elevation data is taken from Algemeen Hoogtebestand Nederland 4 (AHN4, *General Elevation Database of the Netherlands 4*), which has a horizontal resolution of 0.5 m by 0.5 m and a maximum inaccuracy of 3-5 cm. Therefore, the subgrid has a resolution of 0.5 m by 0.5 m (Figure 3).

Buildings are cut from the DEM to prevent water from flowing through them. To prevent the loss of rain that would fall on the building's roofs, all rain potentially falling on buildings is forced directly onto the two nearest manholes. The extent of the resulting DEM forms the base for the friction and infiltration rasters (see Section 3.1.2). Initial surface water levels are set accordingly with the water levels determined by the water board of Delfland (Hoogheemraadschap van Delfland, 2024).

3.1.2 Groundwater (2D)

The initial groundwater level raster used at the start of the simulation is based on historical data. This data is retrieved from Munisense (2024) and is interpolated between the existing groundwater measuring points by using the ordinary Kriging method.

The impervious layer level is usually the bottom of the first aquifer. In the Oostwijk however, the first aquifer is confined by a 17.5 meter thick clay layer, with small layers of sand and peat in between (DINOloket, 2024). The first aquifer itself is mainly composed of sand. Due to the distinction in composition between these two layers, it is decided to include only the confining layer into the model. Therefore, the bottom boundary of the groundwater domain is set to -17 m NAP.

According to van Baaren et al. (2018), vertical groundwater flows in the study area are upwards, which means that the direction of leakage in the model is positive. However, as leakage is a parameter unique to the 3Di software, there are no ref-

erence tables of its values. The initial value of 0.5 mm/day is taken from Kling (2019), who used an early version of the 3Di groundwater module. Although the soil conditions in his study are completely different from the ones in this study, the influence of leakage is assumed to be small enough to apply the same value as an initial quantification.

Local measurements of the porosity and hydraulic conductivity in the Oostwijk are unavailable, so typical values are taken from literature instead. Clay characteristically has a low (0.01 m/day) to very low (0.0001 m/day) hydraulic conductivity (Bot, 2011; Joostdevree.nl, 2024). Still, based on measurements taken north of Vlaardingen, Sman (2015) calibrated the hydraulic conductivity for their groundwater model to be 0.22 m/day. Although this is significantly higher than what is typically expected for clayey soils, a higher hydraulic conductivity is in agreement with the relatively rapid observed reaction time of the groundwater (Munisense, 2024). The initial hydraulic conductivity is therefore set to 0.22 m/day. Sman (2015) also found the effective porosity to be 0.1, which is in the lower end of the range of typical porosity values for clay (Borden, 2006; Woessner & Poeter, 2020) and therefore adopted for this study as well.

Typical values for the Horton infiltration model are available for the SCS soil groups (USACE, 2024). It is assumed that the soil in the study area is of category D (soils with high runoff potential, due to having permanent high groundwater tables and/or being mainly composed of clay). According to Gilliom et al. (2019), this gives an initial infiltration rate of 7.6 mm/h (182.4 mm/day), an equilibrium infiltration rate of 2.5 mm/h (60 mm/day) and a decay rate of 3 hours.

Table 1: Initial values for the groundwater module parameters.

Parameter	Value	Unit
Hydraulic conductivity	0.22	m/day
Porosity	0.10	-
Initial infiltration rate	182.40	mm/day
Equilibrium infiltration rate	60.00	mm/day
Infiltration decay period	3	days
Leakage	0.5	mm/day
Impervious layer level	-17.00	m NAP

3.1.3 Sewerage system (1D)

Dimensions and gradients of all sewers, pumps, overflows and weirs are provided by the municipality of Vlaardinen. To enable exchanges between the leaking sewers and groundwater, the exchange thickness (thickness of the pipe wall) and inward and outward hydraulic conductivity are set for the damaged pipes. The inward and outward hydraulic conductivity are assumed to be equal and to be dependent on the surrounding soil, so a value of 0.22 m/day is set. The used exchange thicknesses are taken from a sewer manufacturer (LBn betonproducten, 2010) and given in Table 2.

Start and stop levels of the pump at the Spoorsingel are provided by the municipality, while the start and stop levels of the Boslaan pumping station are derived from analysis of the measured water levels (see Table 3).

Dry-weather flow (DWF) is all water that flows through the sewerage system that is not rain water. This contains the water flows from daily human activities like taking a shower, doing the dishes or visiting the restroom. As no data on DWF is available for the Oostwijk, a total of 120 liters per person per day is used with a pre-defined distribution over the day (see Figure 5) (RIONED, 2019b). As the number of residents per building is unknown, the total number of inhabitants of the Oostwijk (7400) is divided equally over the number of buildings. The resulting DWF is forced onto the nearest manhole.
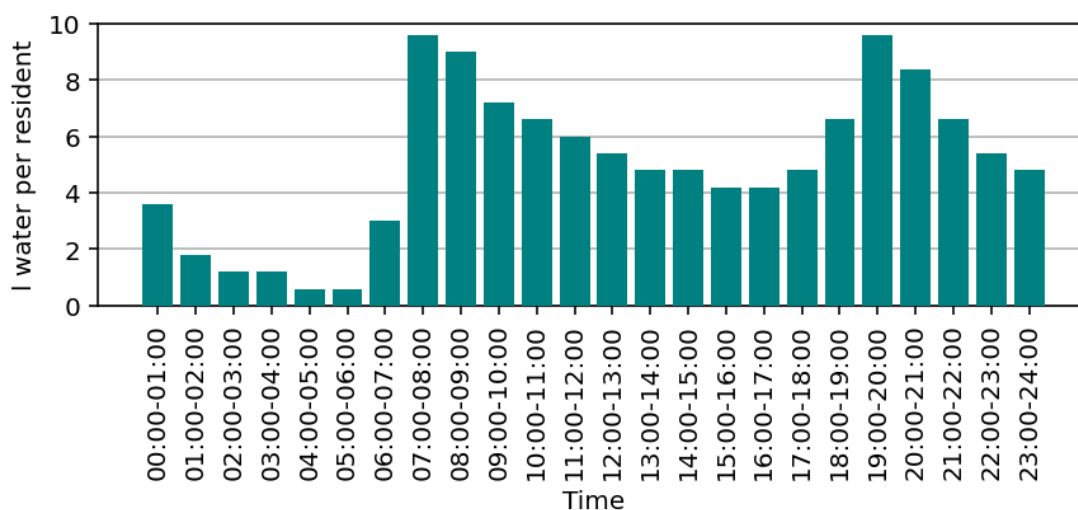
Figure 5: Daily distribution of dry-weather-flow per person as defined by RIONED (2019b).

Table 2: Wall thicknesses of sewers with dimensions present in the Oostwijk (LBn betonproducten, 2010).

Shape	Material	Height/width [mm]	Wall thickness [m]
Circle	Concrete	400/400	0.062
		500/500	0.070
		600/600	0.080 o
		700/700	0.118
		800/800	0.132
		900/900	0.148
		1000/1000	0.165
		1250/1250	0.165
	PVC	315/315	0.009
		400/400	0.012
		500/500	0.014
	Clay	300/300	0.062
Egg	Concrete	600/400	0.100
		900/600	0.110

Table 3: Start and stop levels of the pumps in the Oostwijk

Pump	Start level [m NAP]	Stop level [m NAP]
Spoorsingel	-0.520	-0.620
Boslaan 1	-2.800	-3.250
Boslaan 2	-2.800	-3.250
Boslaan 3	-1.570	-2.800

3.1.4 Boundary conditions

Boundary conditions are applied along the western and eastern boundaries of the model. Along the western part of the model, the water level of the Oude Haven is used as a boundary condition. In the east, at the weir near the Parkweg where surface water leaves the Oostwijk, a water level boundary of -2 m NAP is applied,

to ensure that water can always discharge from the area. For the groundwater model, no boundary conditions are applied (see Section 5.1.1.

3.2   Sensitivity analysis

The uncertainty in the groundwater parameter values is largely due to a lack of measurements in combination with the heterogeneous soil often found in urban areas (Vasenev et al., 2013). To make the calibration process more efficient, a sensitivity analysis is done beforehand to give insight in the relative influence of parameters on the model accuracy. Nine parameters that have single value or are present as a raster in the model are included in this analysis. An overview of these parameters is given in Table 4. Simulations are then run with parameter values ranging from 50% to 150% from their initial values, with increments of 25%pt. Only one parameter is changed per simulation, meaning that with nine parameters included, a total of 45 simulations is run.

Next, the results from each simulation are compared to the measurements (for the used rainfall event, see Section 3.3.2). Groundwater levels were compared to the measurements done at eight of the nine measurement locations. The ninth location (Kortedijk) was excluded from the sensitivity analysis and subsequent calibration due to a systematic measuring error. As the Kortedijk is separated from the main part of the study area by the Oude Haven, this decision is not expected to influence further results. In the sewers, water levels are compared at the Callenburgstraat, the pumping station at the Boslaan and the overflow at the Parkweg (see Figure 1b).

The model accuracy is quantified by using the Kling-Gupta Efficiency (KGE). The KGE is adapted from the in hydrological research widely used Nash-Suthcliffe Efficiency (NSE) and expands on it by also taking statistical bias and variance into account (Clark et al., 2021; Gupta & Kling, 2011). The formula for the KGE is given by Equation 1.

$$\text{KGE} = 1 - \sqrt{(r-1)^2 - \left(\frac{\sigma_{\text{sim}}}{\sigma_{\text{obs}}} - 1\right)^2 + \left(\frac{\mu_{\text{sim}}}{\mu_{\text{obs}}} - 1\right)^2} \qquad (1)$$

Where r is the Pearson's correlation coefficient, σ_{sim} the standard deviation in the simulated data, σ_{obs} the standard deviation in the observed data, μ_{sim} the mean of the simulated data and μ_{obs} the mean of the observed data. The highest possible value of the KGE is 1, at which point the simulated and observed data are equal, i.e. the model shows a perfect fit. If the model accuracy decreases, the KGE

decreases as well. When the KGE drops below -0.41, the model accuracy is so low that taking the mean of the observations is a better predictor than the model (Knoben et al., 2019).

Table 4: Parameters and their values as used in the sensitivity analysis.

Parameter	Abbr.	Initial value	50%	75%	125%	150%
Hydraulic conductivity in/out	P-HC	0.22	0.11	0.17	0.28	0.33
Friction coefficient pipes	P-F	Table	Relative to initial table values			
Friction coefficient surface	S-F	Raster	Relative to initial raster values			
Hydraulic conductivity	G-HC	0.22	0.11	0.17	0.28	0.33
Leakage	G-L	0.50	0.25	0.38	0.63	0.75
Porosity	G-P	0.10	0.05	0.08	0.13	0.15
Initial infiltration	G-II	Raster	Relative to initial raster values			
Equilibrium infiltration	G-IE	Raster	Relative to initial raster values			
Infiltration decay	G-ID	3.00	1.50	2.25	3.75	4.50

3.3   Calibration and validation

3.3.1   Process

As the model will be used to simulate both dry and heavy rain scenarios, the parameter set should be sufficiently robust to be applicable to both conditions. It is therefore chosen to calibrate by using the differential split-sample test, as this method tests the ability of the model to perform during the transition between two conditions by first calibrating on one condition before validating on the other condition (Klemes, 1986). In this study, multiple iterations will be done: first, the model is calibrated on a wet condition, after which it is validated on a dry condition. Based on the model performance after the first iteration, parameter values will be recalibrated on the dry condition before being validated on the wet condition. This process continues until the model results form an acceptable simulation of reality.

Similarly to the sensitivity analysis, the KGE will be used to quantify the model accuracy. This will be done by comparing modelled groundwater levels and water levels in the sewers at the locations mentioned in Section 3.2. However, despite the

fact that the KGE gives excellent insight in the extent to which the pattern of the simulated data follows that of the observations, the KGE is also strongly influenced by the absolute deviation between the observed and simulated values. The Mean Absolute Error (MAE) is used next to the KGE to gain more insight in the absolute values we are dealing with. The MAE gives the sum of the absolute difference of each time step between the simulated and observed data, see Equation 2.

$$\text{MAE} = \frac{\sum_{i=1}^{n} |y_i - x_i|}{n} \tag{2}$$

Where n is the number of observations in the dataset, y is the observed value and x is the simulated value.

The aim of the calibration is to find a model parametrisation which results in an acceptable simulation of reality. Based on what is feasible considering the results of the sensitivity analysis, 'acceptable' is quantified as a KGE of 0.6. With regards to the MAE, the lowest sensible value is the maximum error in the used elevation model, which is 0.03 m. As it is deemed unrealistic to aim for the lowest sensible value, a MAE of 0.06 m is deemed acceptable instead.

Parameters will be tweaked manually in iterations. The parameters which are focused on during calibration, as identified by the sensitivity analysis, are the porosity, initial infiltration and hydraulic conductivity. In addition, the extent to which sewers are leaking is set by altering the exchange thickness of the corresponding pipes. As the chosen parameters mostly influence the groundwater domain and have limited influence on the behaviour of the sewerage system, additional checks are done to ensure the modelled sewerage system resembles the real world system. These include checking the acreage and pumped volumes, comparing the model results to the results shown in the Basic Sewerage Plan (BRP) (el Kajjal & Mogos, 2021) and comparing the reaction of the model on the precipitation input. This last check requires running again for different sources of precipitation input: in addition to data from the NRR, data from the KNMI and a local measurement will also be used.

3.3.2   Used historical rainfall events

Historical events will be simulated during the sensitivity analysis and the calibration and validation phase. To be able to compare the simulations to the corresponding real-life results, the list of possible events is bound by the availability of data. The smallest dataset includes the measurements of water levels in the sewers, which runs from the 30th of December 2022 to the 7th of June 2024. Effectively, this

means that the selected historical events have to be from 2023 and the first half of 2024.

For the rainfall event used in the sensitivity analysis and during calibration, an event with a considerable peak is preferred. Simultaneously, the event should be sufficiently long to be suitable for calibration, as the change in behaviour of the water system should be visible. A duration of two days is expected to be sufficiently long to account for this. Additionally, for the practical purpose of starting with an empty sewer system, the event should ideally have happened after a week without rain. An event meeting all conditions in the given time period is found on the 12th and 13th of October 2023, when 32 mm of rain fell over the span of two days after a week of dry weather. Figure 6 shows the pluviograph of this event over time from three different sources. As mentioned beforehand, data from the NRR is used primarily due to the superior reliability of the data. The data from the KNMI and the local source are used only to check the reliability of the reaction of the model of the sewerage system on different precipitation inputs.
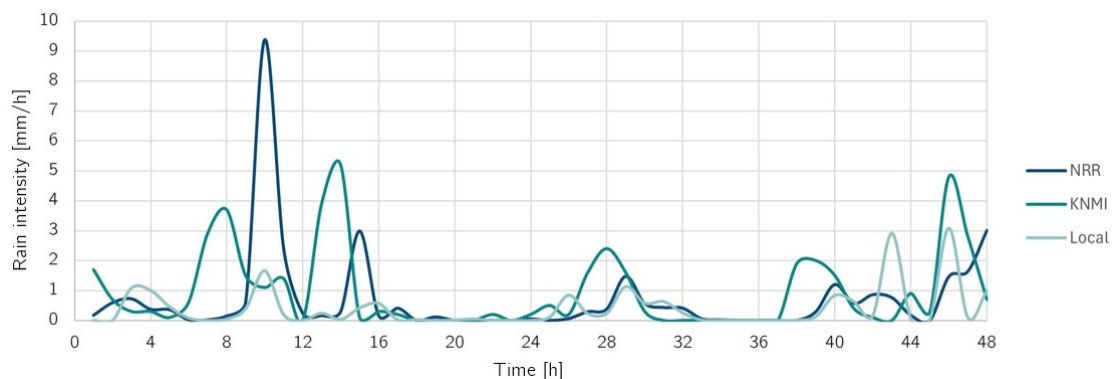
Figure 6: The rainfall on 12-13th of October 2023 as given by the NRR, KNMI and a local measurement.

A dry event is also used for calibration and validation. For this, seven subsequent days without rain are searched for in the given time frame. The dry week before the chosen rainfall event is excluded to prevent over-calibrating. Finally, the period from the 9th to the 17th of June 2023 is chosen as the dry event.

3.4 Analysis of the effects of rainfall on the model

3.4.1 Process

To investigate the consequences of the more intense rainfall in the future on the study area in its current condition, a future rainfall event is put on the calibrated model. For this, the initial groundwater level raster is made from the average groundwater levels over the last four years. All other parameters are kept equal to the calibrated ones.

To analyse the effects of the rainfall event on the study area, several indicators are considered. Pluvial flooding is indicated by the flood duration of maximum water depth on the streets, as well as by the number of vulnerable buildings. Flooding depths and durations are measured at eight locations in the south of the Oostwijk (see Figure 7). Vulnerable buildings are derived by the advanced method based on DGBC (2023), where buildings are classified in either having no-risk, low-risk (0-10 cm), mid-risk (10-25 cm) or high-risk (>25 cm) of having water standing above floor level. Groundwater fluctuations are regarded through the standard deviation in the groundwater level over time. Additionally, to gain general insight into the water distribution in the Oostwijk, the water balance of the study area is considered.

Figure 7: Locations at which maximum depth and duration of pluvial flooding are measured.

3.4.2 Used future rainfall event

Currently, the municipality of Vlaardingen assesses their sewerage by using Bui08, which has a present day return time of 2 years (RIONED, 2019a). However, as our interest is not just limited to sewerage and instead compasses surface runoff and groundwater as well, in addition to the scope of the study extending to future climate, Bui08 is not suited to assess the proposed measures. Instead, a composite rainfall event is used, as this type of rainfall event is applicable for both sewerage and surface water calculations (Vaes & Berlamont, 1996). A series of composite rainfall events for future climate scenarios has been derived by RIONED (2020). Although these events are based on climate scenarios for 2014 as developed by the KNMI (2014), a recent study found them to still be compliant with today's climate projections (STOWA, 2023). It is chosen to work with the most severe climate scenario to increase the robustness of the solutions and a temporal scope of 2050 is chosen in consultation with the municipality. Likewise, the return time of the rainfall event is chosen to be similar to the return time of Bui08, thus being 2 years. Together, this leads to the rainfall event used to assess the scenarios being the composite rainfall event with a return time of 2 years for the W_H climate scenario in 2050. This event has a duration of 10 hours, a total volume of 43.5 mm and an intensity of 89 mm/h at its peak. The corresponding pluviograph is shown in Figure 8.

The used rainfall event is followed by 6 days and 14 hours of dry weather, which allows the groundwater system to react to the precipitation so conclusions on the changes in groundwater over time can be drawn. This makes that the total simulated time is 7 days.

3.5 Addition of measures to the model

To answer the third research question, a canal will be implemented into the model. This canal is added in 2D. It is connected to the existing water bodies in the Oostwijk by culverts: to the Oranjepark in the north and the Spoorsingel in the south. Both culverts have a diameter of 400 mm.

3.5.1 Scenarios

Canal length Three length variants of the canal are simulated to investigate the influence of the canal length on the effects of adding the canal. The shortest variant of the canal (*L1*) has a length of 125 meter and is located where the Binnensingel has the lowest elevation; between the intersections with the Willem
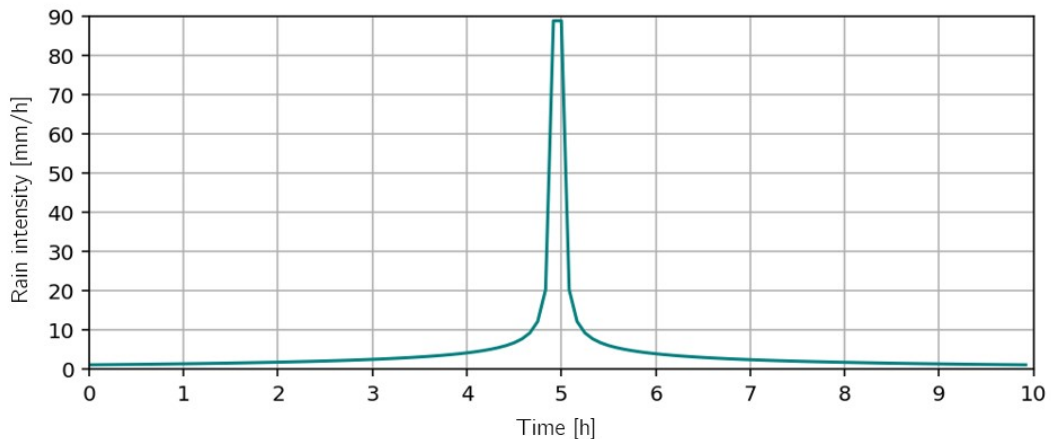
Figure 8: Pluviograph of the used composite rainfall event, which has a return time of 2 years for a 2050 climate scenario.

Beukelszoonstraat and the Oosterstraat (see Figure 10a). In the second length variant (*L2*), this canal is expanded to the roundabout in the north and to the intersection with the 2e van Leyden Gaelstraat in the south, leading to a total length of 251 meter (Figure 10b). The third and longest variant (*L3)* comprises the entire Binnensingel between the roundabout and the Spoorsingel with a length of 370 meter (Figure 10c)

Water level   The canal is located within a fixed water level area with water level -0.57 m NAP (see Figure 1c). Sticking to this water level does however force the groundwater level upwards to a significant extent (see Figure 9), which enlarges the risk of groundwater hindrance. It is therefore interesting to explore the option of lowering the prescribed surface water level. This chosen lowered water level is -0.80 m NAP, as this is closer to the average groundwater level along the Binnensingel, as well as being the lowest surface elevation in the surrounding area (the Willem Barendszoonstraat). In the scenarios with this lower water level, the water level of the Spoorsingel is lowered to -0.80 m NAP as well.

Disconnecting   Adding a canal only makes sense when the additional storage and influence on groundwater can be used, so the canal should be filled during rainfall. To achieve this, the street and front roofs of the buildings along the canal are disconnected (see Figures 10a-10c). However, adding a canal theoretically gives the potential to increase the disconnected area. To investigate whether this is a possibility, the streets and renovated houses in the Zeevaardersbuurt, a planned redevelopment east of the Binnensingel, are disconnected in addition to the streets
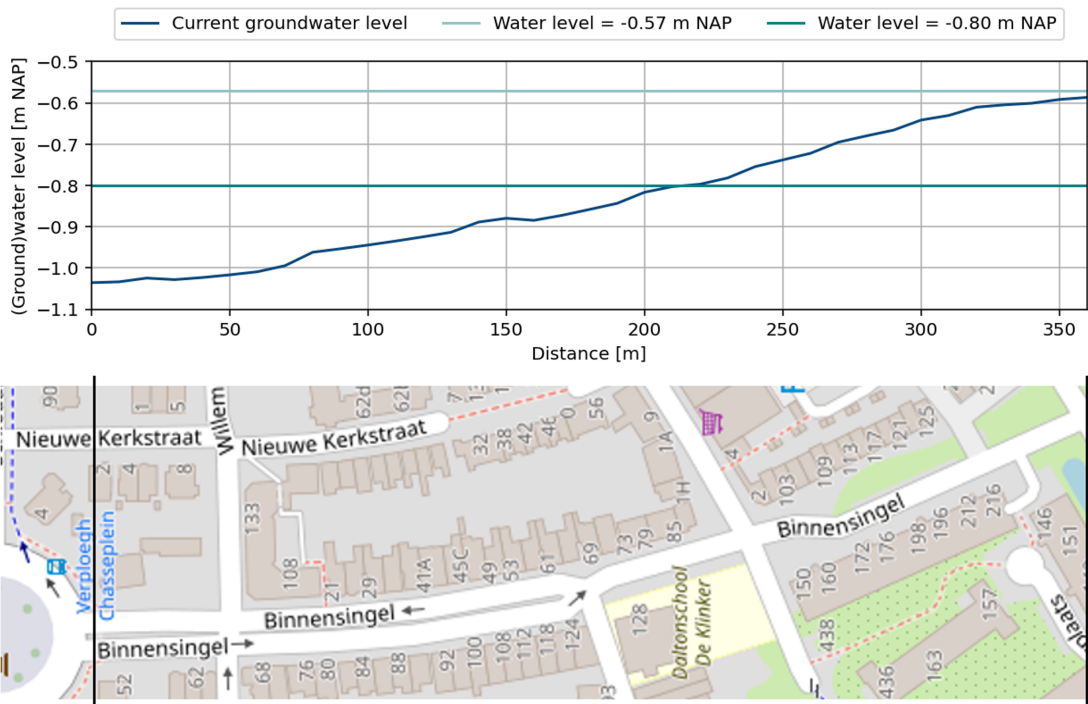
Figure 9: Groundwater levels along the Binnensingel in the current situation compared with the scenarios with the full-length canal with water levels of -0.57 m NAP and -0.80 m NAP.

and roofs along the canal (see Figures 10d-10f). While for the smaller disconnected area water can freely flow over the surface, the larger variant requires rainwater sewerage to transport water towards the canal. As no design for this has been made by the municipality and designing a full sewerage system is not part of the scope of this study, a simple sewerage system with a constant slope of 1/1000 and a constant diameter of 400 mm is added to the model. At the end of this system, water is pumped into the canal at two locations by pumps with a capacity of 16.7 l/s (similar pumps to the one at the Spoorsingel).

With three variants of the length of the canal, two variants of the water level in the canal and two variants of disconnected area, a total of twelve scenarios are created. Table 5 gives an overview of the scenarios and the corresponding scenario codes used in this study.

(a) L1-Ak   (b) L2-Ak   (c) L3-Ak

(d) L1-Ag   (e) L2-Ag   (f) L3-Ag
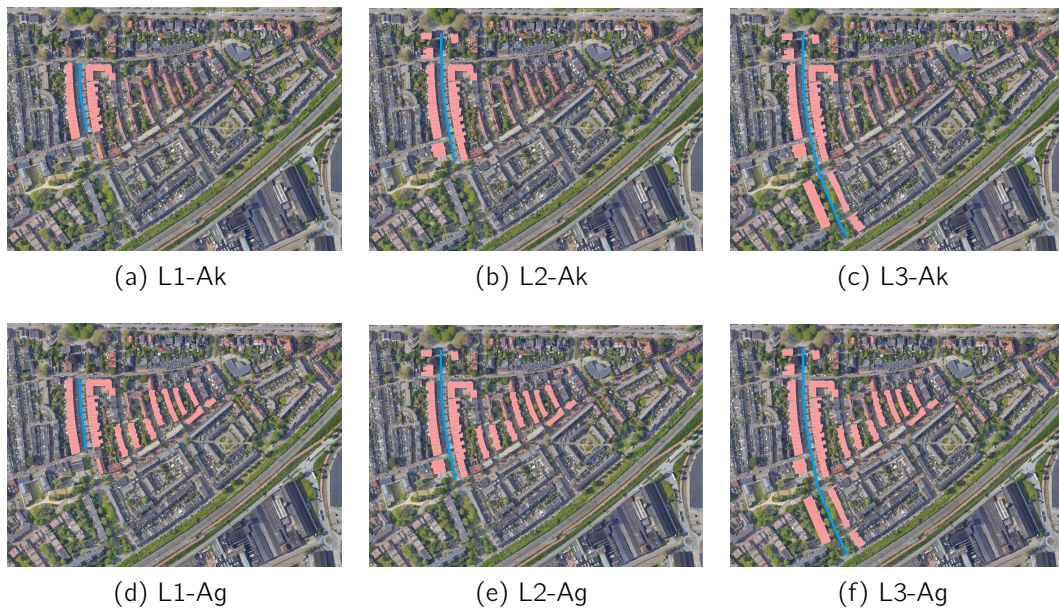
Figure 10: Overview of the different disconnecting scenarios. The pink shapes are disconnected buildings. The blue lines indicate the canal lengths, in which L1 is the shortest and L3 the longest version. Ak and Ag stand for the small and large extent of disconnecting,respectively.

3.5.2   Initial groundwater levels for scenarios

Running the model with the added surface water and the original initial groundwater levels raster predictably causes the groundwater levels around the added canal to rise as already visible in Figure 9. As we are interested only in the change in groundwater behaviour after a new equilibrium has been set, either simulations should start with a warm-up period, or the initial conditions should be changed. In tests, it is found that the length of the warm-up period should be approximately 4 days. This would however increase the (already long) total simulation time by almost 60%. It is therefore chosen to revise the initial groundwater level raster by including the canal (and thus the water level) in the interpolation procedure.

Table 5: Overview of the scenarios. L1, L2 and L3 stand for canal length 1, 2 and 3 respectively. Ak and Ag stand for the small and large extent of disconnecting respectively. WP057 stands for a canal water level of -0.57 m NAP and WP080 stands for a canal water level of -0.80 m NAP.

Canal length	Water level	Disconnecting	Code
Length 1	-0.57	Small extent	L1-Ak-WP057
		Large extent	L1-Ag-WP057
	-0.80	Small extent	L1-Ak-WP080
		Large extent	L1-Ag-WP080
Length 2	-0.57	Small extent	L2-Ak-WP057
		Large extent	L2-Ag-WP057
	-0.80	Small extent	L2-Ak-WP080
		Large extent	L2-Ag-WP080
Length 3	-0.57	Small extent	L3-Ak-WP057
		Large extent	L3-Ag-WP057
	-0.80	Small extent	L3-Ak-WP080
		Large extent	L3-Ag-WP080

4 Results

4.1 Sensitivity analysis

4.1.1 Groundwater

For groundwater, Figure 11 shows that the results of the simulation with the initial parameter values (100%) lead to a KGE of -0.22, which is far from an acceptable simulation of reality. Three parameters seem to have visible influence on the model fit. These are the initial infiltration, of which a higher value results in a better model fit, and the hydraulic conductivity and porosity of the soil, for both of which a lower value results in a better model fit. This effect is the largest for the porosity.

Combined these three dominant parameters indicate that for the initial values the model simulates a water level that is too low: contrary to what the groundwater level measurements show, the modelled groundwater level barely rises after rainfall. This is caused by too little infiltration, as the KGE increases for a higher initial infiltration, by too much storage, as the KGE increases for lower porosity, and by excessively quick flow velocities, as the KGE increases for lower hydraulic conductivity.

Based on the sensitivity analysis, it is decided to calibrate by focussing on the initial infiltration, porosity and hydraulic conductivity. It must be noted that especially the porosity and hydraulic conductivity often go together: a more poreus soil is also likely to have a higher permeability, so calibrating on both parameters is physically sensible.
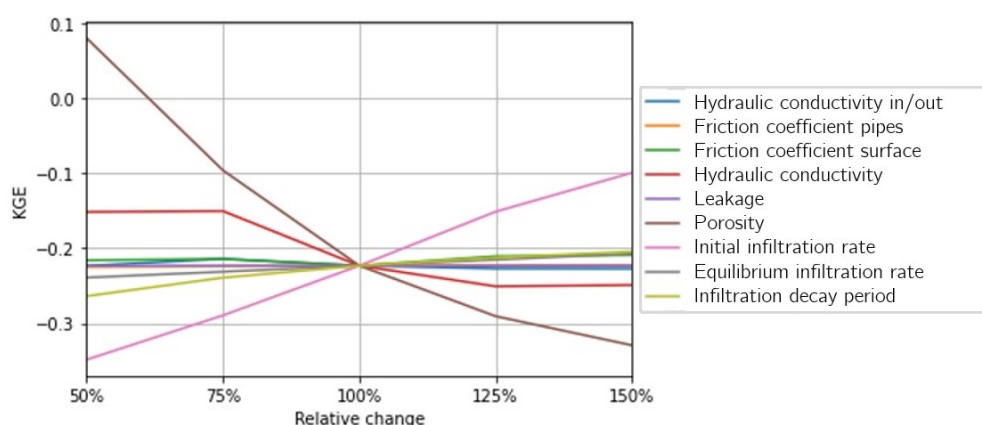
Figure 11: Influence of parameters on the accuracy of the groundwater model, indicated by the KGE.

4.1.2   Sewerage system

Figure 12 shows that the base scenario has a KGE of -0.28 for the sewerage system, which means that the model results for the sewerage system are even worse than those for the groundwater model. In the tested range, most of the included parameters seem to have little influence on the correlation between the observed and simulated water levels. The exception to this is the initial infiltration, of which a higher value results in a slightly better prediction of the water level in the sewerage system. This can be explained by the fact that higher infiltration values limit the amount of surface flow and therefore the inflow into the sewerage system. This effect is the strongest for the initial infiltration, as this is the infiltration parameter that has an immediate effect at the start of the model.

In general, the results show that for the initial values the model simulates too much flow in the sewer system. Yet, the very low KGE values and the small change in KGE over different parameter inputs indicate that the simulated flow in the sewerage system is likely to follow a different pattern when compared to measurements. Possible reasons for this are a differences between the fallen rainfall and the precipitation input on the model or measurement errors.
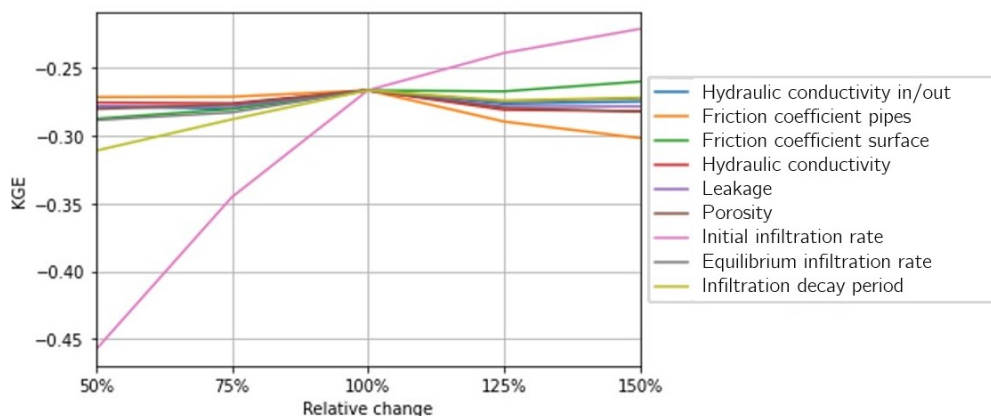
Figure 12: Influence of parameters on the model accuracy of the model of the sewerage system, indicated by the KGE.

4.2 Calibration and validation

4.2.1 Groundwater

The final values for the parameters of the groundwater module are shown in Table 7, while Table 6 gives the values of the objective functions for each of the groundwater measurement points after calibration and validation. On average, the groundwater domain of the model achieves a KGE of 0.585, which is just below the aim of 0.6. One major outlier in the KGE values for the individual groundwater measurement points is found at the Hogelaan in the dry condition (for an explanation of this point, see Section 5.1.1). When excluding this point, the average KGE for the groundwater domain is 0.715, which is well above the aim of 0.6. The MAE does not show any significant outliers and has an average of 0.039 meter in the groundwater domain, which is well below the allowed maximum of 0.06 meter.

Table 6: Objective functions indicating the accuracy of the modelled groundwater levels at eight locations in both wet and dry conditions after calibration and validation.

	Wet condition		Dry condition	
Location	KGE	MAE [m]	KGE	MAE [m]
Hogelaan	0.871	0.101	-1.135	0.025
2e Maasbosstraat	0.632	0.053	0.813	0.004
1e Van Leyden Gaelstraat	0.151	0.165	0.771	0.009
Nieuwstraat	0.974	0.011	0.857	0.025
Callenburgstraat	0.841	0.041	0.752	0.012
Schiedamseweg	0.842	0.008	0.297	0.008
Emmastraat	0.865	0.057	0.656	0.020
Average	0.739	0.062	0.430	0.015
Average (both wet and dry)	KGE: 0.585		MAE: 0.039	

4.2.2 Sewerage system

The final values of the parameters regarding the sewerage system are shown in Table 7, while the values of the objective functions for the sewerage are given in Table 8.

Table 7: Calibrated values for the groundwater model parameters. 100% with respect to initial means that the value did not change compared to the initial value.

Parameter	Value	Unit	w.r.t initial
Hydraulic conductivity in/out	0.02	mm/day	10%
Friction coefficient pipes	0.01	$s/m^{1/3}$	100%
Friction coefficient surface	Max: 182.6	-	100%
Hydraulic conductivity	0.11	m/day	50%
Leakage	0.5	mm/day	100%
Porosity	0.05	-	50%
Initial infiltration rate	273.60	mm/day	150%
Equilibrium infiltration rate	60.00	mm/day	100%
Infiltration decay period	1	days	33%

The objective functions indicate that the model cannot accurately simulate reality. The KGE is far below the required value of 0.6 at all three locations for both wet and dry scenarios. Values for the MAE are satisfactory for the Callenburgstraat and Parkweg in the dry scenario only, which indicates that the model simulates the DWF correctly, but has trouble simulating the rainfall runoff. The very bad MAE values at the Boslaan underline this.

Table 8: Objective functions indicating the accuracy of modelled water levels in the sewerage system in both wet and dry conditions after calibration and validation.

Location	Wet condition		Dry condition	
	KGE	MAE	KGE	MAE
Callenburgstraat	-0.422	0.028	0.019	0.011
Parkweg	0.005	0.041	0.047	0.017
Boslaan	0.288	0.199	-0.097	0.150
Average	-0.043	0.089	-0.010	0.059
Average (both wet and dry)	KGE: -0.27		MAE: 0.073	

Contrary to the objective functions, the additional checks draw a more positive view of the sewerage system model. The acreage of the model (18.86 acres of roofs and 19.34 acres of impervious area) resembles that of the model used in the BRP (18.90 acres of roofs and 18.80 acres of impervious area). The model also reacts well to different input sources: the pattern of the simulated flow in the sewers directly resembles the pattern of the precipitation input. It is noteworthy that the flow in the sewers simulated with the local measurement as input comes close to the measured flow (see Figure 13).
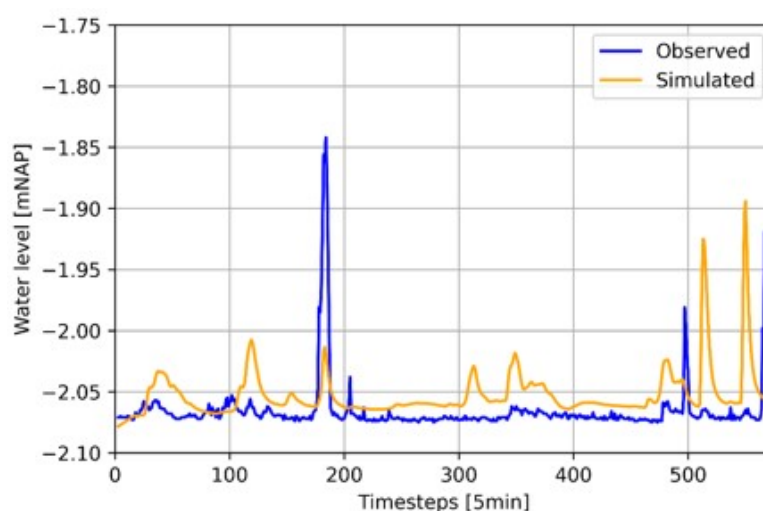
Figure 13: Measured and simulated flow in the sewer below the Callenburgstraat on the 12th and 13th of October 2023. Note how the simulated flow closely resembles the locally measured precipitation in Figure 6.

Pumped volumes from pumping station Boslaan are calculated for simulations with input rainfall from the NRR, KNMI and the local measurement. These volumes are compared to the theoretical maximum pumped volume, which is the pumped volume if all pumps would have worked on 100% capacity during the entire period they were active. The comparison is shown in Figure 14. Large differences between the input sources can be seen: with the KNMI input, more pumped volume is calculated than theoretically possible, while with the local input, only about half of the theoretical maximum is discharged. Importantly, pump 3 does not activate for either of these input sources, while having been active in the measurements. With rainfall input from the NRR, pump 3 does activate, but the cumulative volume from all pumps is 2500 m^3 lower than the theoretical maximum. This is however realistic, as the pumps are unlikely to have pumped at full capacity during the entire time they were active.
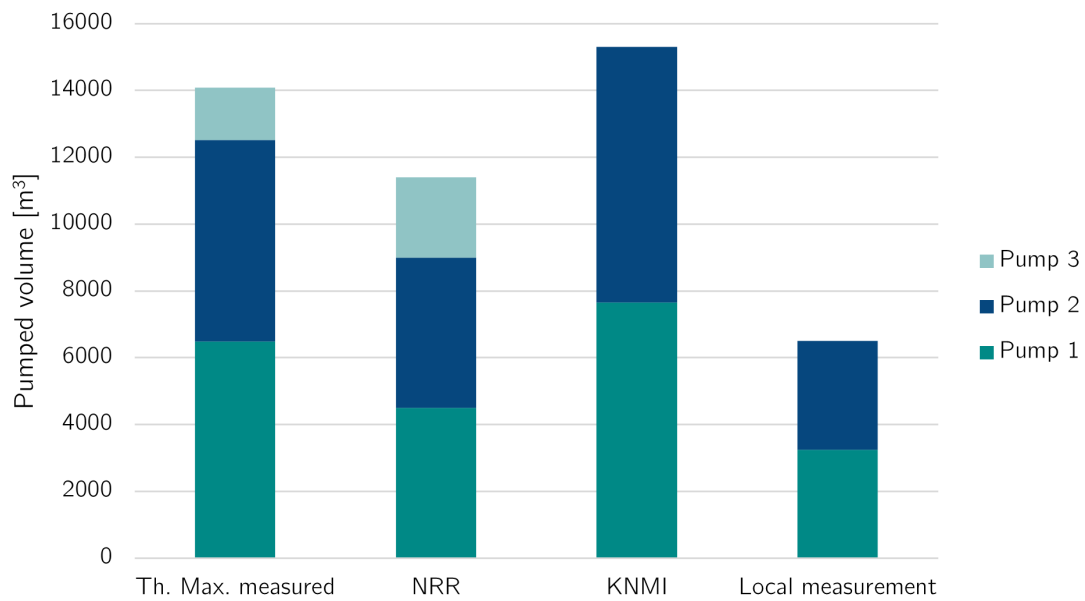
Figure 14: The theoretical maximum measured pumped volume at pumping station Boslaan compared to the volumes calculated by the model for different precipitation input sources.
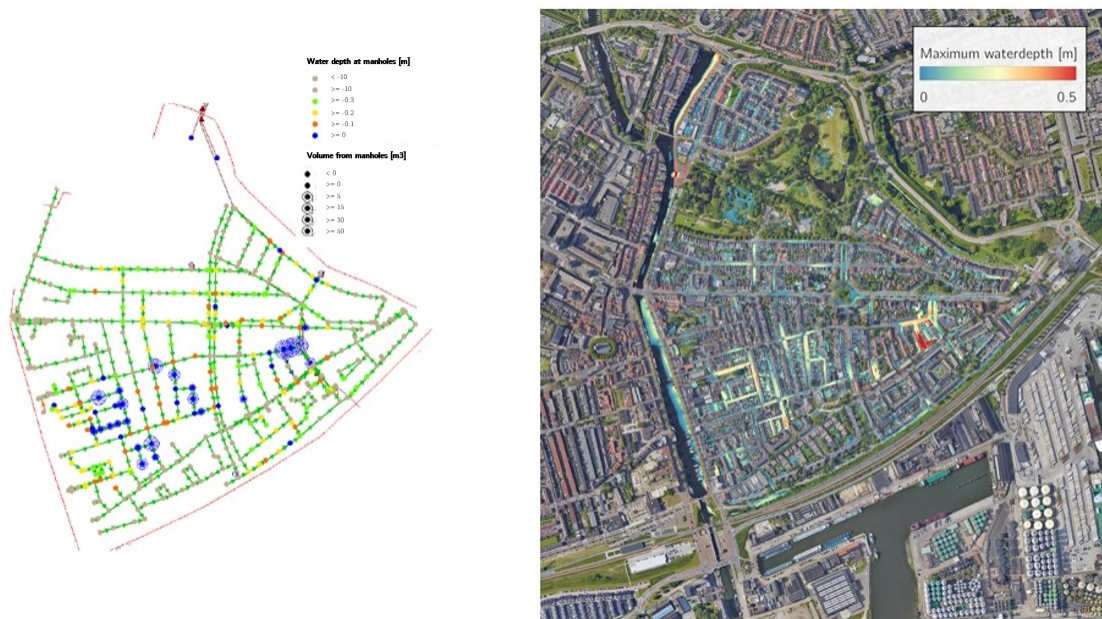
Figure 15: Pluvial flooding as calculated in the BRP (left) and the model used in this study (right). In the latter, pluvial flooding is also calculated on the Oude Haven, along the left side of the model. This is because the Oude Haven has not been modelled in 2D, so excess water above its standard water level is shown as pluvial flooding on the map. In reality, this water is safely stored as surface water in the Oude Haven.

Finally, when running the model with Bui08, the calculated amount of pluvial flooding resembles that of the model used in the BRP (see Figure 15). While the result from the BRP (left part of the figure) is shown as the hydraulic head at each manhole and the result from the model (right part of the figure) is shown as water depth on the surface, the locations in which pluvial flooding occurs are similar in both images.

Due to the large differences the locally measured precipitation has shown compared to precipitation measured by the KNMI and the NRR and the very low pumped volume calculated with the local precipitation input, while the calculated flow resembles the measured flow, it is expected that the sensor measuring both precipitation and water level have low accuracy. As these measurements are the only data to which the model output can be compared, it is hard to quantify the accuracy of the model. Still, in the additional checks, the model has shown to react fast and reliably on different precipitation inputs and to be able to recreate results from the BRP. The model of the sewerage system is therefore deemed to be sufficiently accurate for usage in this study.

4.3   Effects of future rainfall event on the current situation

4.3.1   Pluvial flooding

Table 9 shows the maximum water depth and flood duration at eight locations in the study area for the current situation, while Figure 16 shows this on a map. It can be seen that pluvial flooding occurs throughout the entirety of the Oostwijk. The heaviest pluvial flooding does however occur in the subsided areas south of the Schiedamseweg. West of the Binnensingel, standing water has a maximum depth of approximately 30 cm and it takes 2 hours and 15 minutes for this water to be discharged. The extent of pluvial flooding is similar on the east of the Binnensingel, with the exception of the Willem Barendszoonstraat, where the maximum water depth reaches 67 cm and has a duration of 3 hours and 20 minutes. Overall, this amount of pluvial flooding exceeds the maximum allowable effects of a maximum of 20 cm of water for a maximum duration of 1 hour in residential streets.

4.3.2   Vulnerable buildings

Figure 18 shows the buildings which in the current situation are calculated as vulnerable to flooding under the future rainfall event. Of the total of 2964 buildings in the Oostwijk, 948 buidings are calculated to be vulnerable, of which 610 are low-risk, 209 mid-risk and 129 high-risk. Virtually all these buildings are either houses

Table 9: *Duration and maximum depth of pluvial flooding at eight locations after a T2 2050 composite rainfall event. Duration is given in hh:mm, depth in m.*

Location	Duration	Depth	Location	Duration	Depth
Willem Barendszoonstraat	03:20	0.67	Binnensingel	02:00	0.25
Willem Beukelszoonstraat	02:35	0.29	Wilhelminastraat	02:15	0.25
Boslaan	02:15	0.20	Callenburgstraat	02:15	0.36
Nieuwe Kerkstraat	02:15	0.25	Eendrachtstraat	02:15	0.32

Figure 16: *Maximum depth of pluvial flooding after a T2 2050 composite rainfall event. The eight measuring locations are the ones shown in Figure 7. Values of the measurements are given in Table 9.*
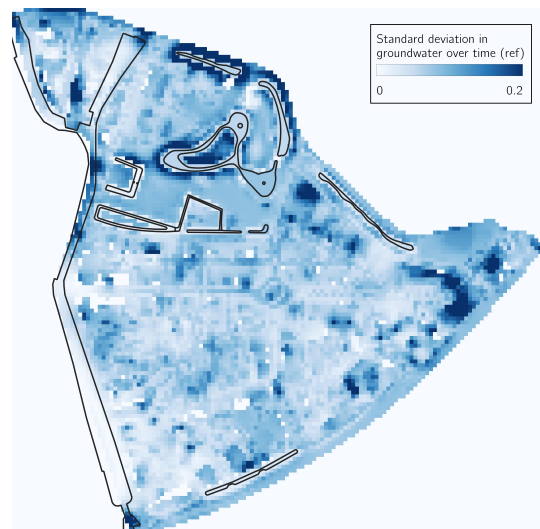
Figure 17: *Raster showing the standard deviation in the groundwater level over time for every grid cell. A darker colour indicates more groundwater fluctuation. The outlines of the open water bodies are shown.*

or apartment blocks, although the few exceptions (a school, an office building and metro station) are all calculated to have high risk vulnerability. Generally, high-risk buildings are located in roughly three locations. The first is around the Willem Barendszoonstraat, which coincides with the large water depths during flooding in this street (see Section 4.3.1). The second location is in the eastern corner of the Oostwijk, where water accumulates in the backyards of the vulnerable buildings. The third location is along the Oude Haven. Although the backs of these buildings are located significantly lower than the front facades, little water is seen ponding in the backyards. In consultation with the municipality, it is found that these buildings

have historically not been vulnerable. Their classification could therefore be an artefact from the used method (see Section 5.1.2). Most of the mid-risk buildings are located in the subsided areas around the Eendrachtstraat and Wilhelminastraat, the locations of which overlap with those where standing water is calculated (see Section 4.3.1).
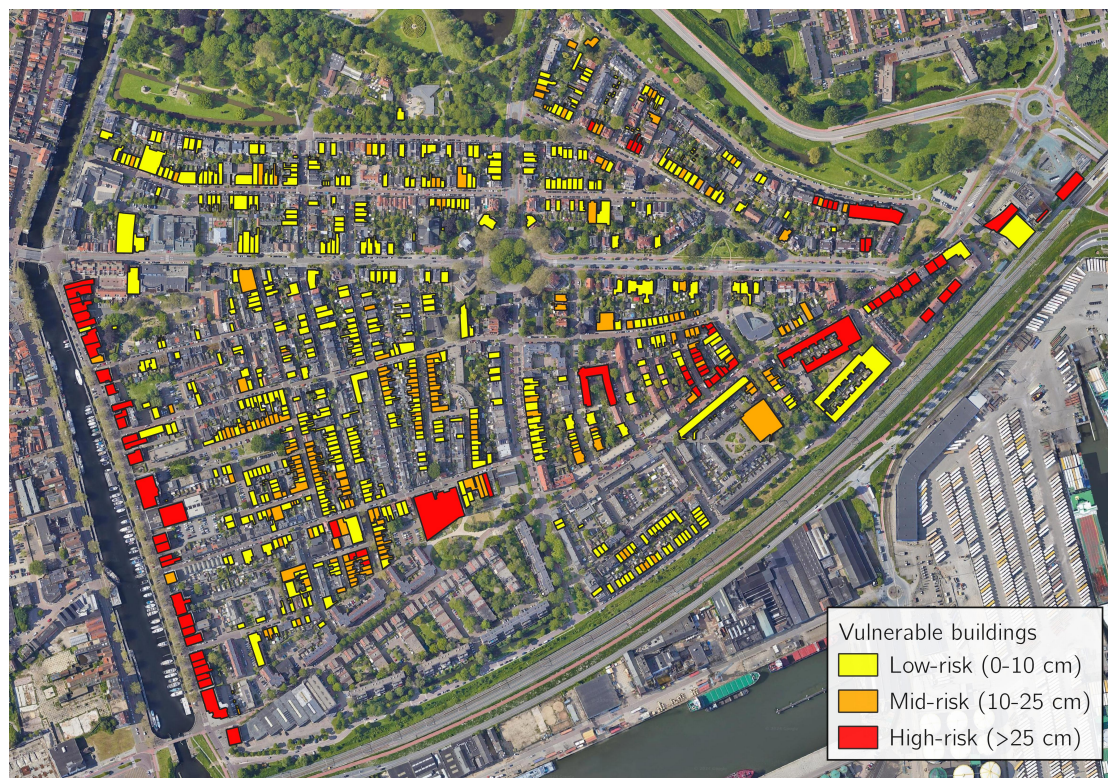
Figure 18: Buildings indicated as vulnerable to flooding by the model after a T2 2050 composite rainfall event.

4.3.3 Water balance

Figure 19 shows the water balance of the Oostwijk in the current situation over the simulated time, with the inflow split into stored and discharged terms. The terms in the water balance entail the following:

- Total inflow: the cumulative volume added to the study area during the simulation time. The total inflow is a combination of:
  - Rain: all rain falling on the study area (both surface and roofs)
  - DWF: dry-weather flow from buildings into the sewerage system

- Surface water: water flowing into the study area from the outside, for example the constant flow from the Oude Haven to the Spoorsingel
- Total Δ stored: the change in the amount of water stored in the study area during the simulation time. The total Δ stored volume is a combination of:
  - Δ sewerage storage: change in the amount of water stored inside the sewerage system
  - Δ surface water storage: change in the amount of water stored as surface water. For example: the ponds in the Oranjepark
  - Δ groundwater storage: change in the amount of water stored as groundwater. This value is equal to the net infiltration.
- Total discharged: the cumulative volume discharged from the study area during the simulation time. To total discharged volume is a combination of:
  - To sewage treatment plant: water pumped from the study area towards the sewage treatment plant.
  - To Nieuwe Maas: all water pumped directly to the Nieuwe Maas by the overflow pump at the Boslaan, which activates due to the large amount of simulated rain.
  - To other waterways: discharge from the study area via other routes. For example: water from the Spoorsingel being pumped back to the Oude Haven, or water flowing over the weir at the Parkweg.

4.3.4   Groundwater fluctuations

Figure 17 shows for every computational grid cell the standard deviation in groundwater level over the simulation time. The largest standard deviations are found along the edges of the ponds in the Oranjepark with a standard deviation of 20 cm and higher. At the locations of the ponds themselves, the standard deviation is equal across the entire water body, yet not 0. Both these observations can be traced back to the rising water level in these ponds, which force the groundwater level to go upwards as well. The water level in the ponds rapidly decreases to its equilibrium again as water is discharged from the study area, which limits the standard deviation on these locations. The groundwater flows along the edges of the ponds are slower, which leads to larger standard deviations.

In the south of the Oostwijk, locations with leaking sewerage are also shown to have higher standard deviations in the groundwater level. Yet, these deviations appear to be very local. Outside of these locations, the standard deviation in groundwater levels is in the range of 0 to 0.1 m.
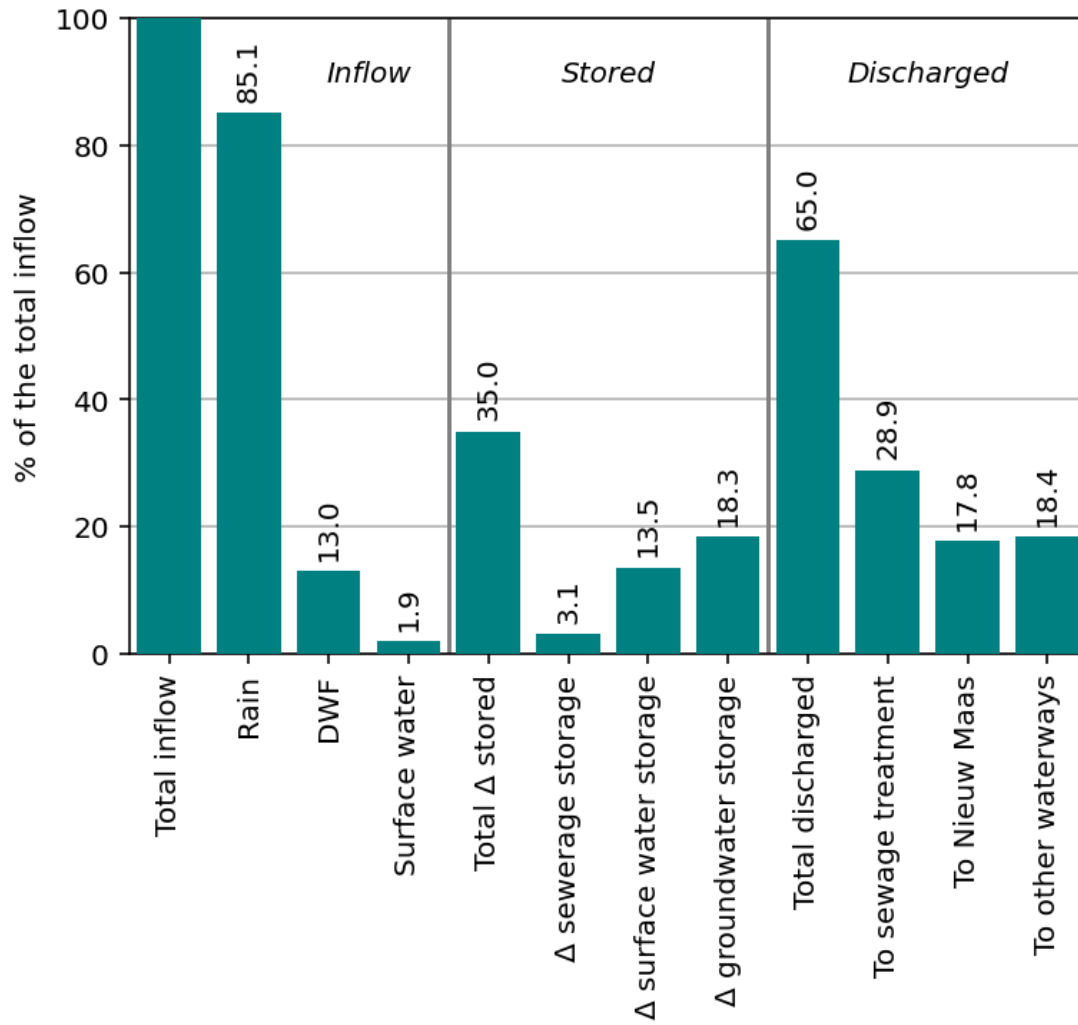
Figure 19: Water balance of the current situation for a T2 2050 composite rainfall event followed by a week without precipitation.

4.4 The effects of a future rainfall event on the scenarios

4.4.1 Pluvial flooding

In Table 10, the duration of water on the street and maximum water depth at each pluvial flooding location is shown for all scenarios.

Firstly, it must be noted that all differences are small: in the range of minutes for the durations, and in the range of centimeters for water depths. Secondly, we can group the eight locations in three groups: 1) the Binnensingel 2) the locations within the Zeevaardersbuurt (Willem Barendszoonstraat, Willem Beukelszoonstraat and Nieuwe Kerkstraat) and 3) the other locations.

At the Binnensingel, the time during which water flows from the manholes is reduced to zero when a canal is added. Still, some ponding takes place next to the canal, although this is greatly reduced in depth. The extent of this reduction depends on the amount of storage added in the canal in combination with the extent of disconnecting. For every increase in length, the water depth is decreased by 5 cm, while lowering the water level in the canal leads to a reduction in water depth on the street of 17 cm. When the Zeevaardersbuurt is disconnected, the water depth is increased by approximately 5 cm compared to the same scenario without this disconnection, which indicates that the storage added by the canal and the added rain water sewer is not sufficient to account for the disconnection. This storage only becomes sufficient when the canal is of at least length 2 (250 m) and the water level is -0.80 m NAP.

At the locations in the Zeevaardersbuurt, the water depth does not significantly change between the scenarios. However, the duration is decreased by 5 minutes for every increase in canal length in the scenarios in which this area is not disconnected. In the scenarios in which the Zeevaardersbuurt is disconnected, the duration of pluvial flooding increases by approximately half an hour and is rather constant between the scenarios. This indicates that the implemented rain water sewer has less discharging capacity than the original combined sewer, which is caused by the fact that once the water level in the canal exceeds the height at which the rain sewer connects to the canal, water from the sewer cannot discharge into the canal anymore. The exception to this is the Nieuwe Kerkstraat, where the duration of pluvial flooding is decreased by almost an hour when disconnected. This likely indicates an influence of the surface elevation as well, as the Nieuwe Kerkstraat has a higher elevation than the Willem Barendszoonstraat.

At the other locations, the water depth is once again more or less constant across all scenarios. It is however notable that the duration of pluvial flooding at these locations decreases in the scenarios in which the Zeevaardersbuurt is disconnected, despite these locations not actually being part of this area. In fact, only the Boslaan is located even close to the Zeevaardersbuurt, with the other three being part of the western part of the Oostwijk. This effect can be explained by the fact that the disconnection of the Zeevaardersbuurt decreases the amount of water that flows into the combined sewerage system, thus creating more storage space for water from upstream locations and therefore decreasing the time upstream locations are flooded.

4.4.2 Vulnerable buildings

Table 11 gives an overview of the number of vulnerable buildings for all scenarios. It can be seen that the numbers are relatively equal across the scenarios, indicating that neither the addition of the canal or disconnecting has much of an influence on the vulnerability of buildings. The scenario with the largest decrease in vulnerable buildings is L3-Ag-WP057, in which 19 houses are less vulnerable than in the current situation. All 19 of these buildings are low-risk in the current situation. Two of the buildings that currently are high-risk and 11 that are mid-risk have changed to mid-risk and low-risk respectively. Although all buildings with decreased vulnerability are located south of the Schiedamseweg, no connection between the number of buildings with decreased vulnerability and distance to the canal is found. Once again, this can be explained by the disconnection of the Zeevaardersbuurt having decreased maximum water depths elsewhere in the study area.

4.4.3 Water balance

To give insight in the effects of the implemented measures on the water balance, Table 12 shows the relative changes in the water balance terms for all scenarios compared to the current situation, with the optimal values highlighted in blue. Overall, scenario L3-Ag-WP080 shows the largest changes. Compared to the reference, an additional 3.1%pt of water is stored in this scenario. Almost half of this water is stored on the surface, almost another half is infiltrated into the soil and the remainder (0.2%pt) is stored in the sewerage system. Where the storage increases, the discharge logically decreases with the same amount. Discharge to the sewage treatment plant, the Nieuwe Maas and to other waterways is decreased rather equally.

Table 10: Duration and depth of pluvial flooding at eight locations for all scenarios. The lowest values are highlighted in blue. Duration is given in hh:mm, depth in m.

Location		Reference	L1-Ak-WP057	L1-Ag-WP057	L1-Ak-WP080	L1-Ag-WP080	L2-Ak-WP057	L2-Ag-WP057	L2-Ak-WP080	L2-Ag-WP080	L3-Ak-WP057	L3-Ag-WP057	L3-Ak-WP080	L3-Ag-WP080
Willem Barendszoonstraat	Duration	03:20	03:20	03:50	03:15	03:45	03:10	03:50	03:15	03:45	03:10	03:45	03:10	03:45
	Depth	0.67	0.67	0.66	0.66	0.66	0.66	0.65	0.66	0.66	0.66	0.65	0.66	0.65
Willem Beukelszoonstraat	Duration	02:35	02:30	03:05	02:30	03:00	02:30	03:05	02:30	03:00	02:30	03:00	02:30	03:00
	Depth	0.29	0.29	0.28	0.28	0.28	0.28	0.27	0.28	0.27	0.28	0.27	0.28	0.27
Boslaan	Duration	02:15	02:10	01:55	02:10	01:55	02:10	01:55	02:10	01:55	02:10	01:55	02:10	01:55
	Depth	0.20	0.19	0.19	0.19	0.19	0.19	0.18	0.19	0.19	0.19	0.18	0.19	0.18
Nieuwe Kerkstraat	Duration	02:15	02:10	01:20	02:10	01:10	02:10	01:10	02:10	01:10	02:05	01:10	02:05	01:10
	Depth	0.25	0.24	0.22	0.24	0.22	0.24	0.21	0.24	0.21	0.24	0.21	0.24	0.21
Binnensingel	Duration	02:00	00:00	00:00	00:00	00:00	00:00	00:00	00:00	00:00	00:00	00:00	00:00	00:00
	Depth	0.25	0.15	0.20	0.00	0.03	0.10	0.15	0.00	0.00	0.07	0.10	0.00	0.00
Wilhelminastraat	Duration	02:15	02:10	02:00	02:10	02:00	02:10	02:00	02:10	02:00	02:05	02:00	02:05	02:00
	Depth	0.25	0.25	0.25	0.25	0.25	0.25	0.24	0.25	0.24	0.25	0.24	0.25	0.24
Callenburgstraat	Duration	02:15	02:15	02:05	02:10	02:05	02:10	02:00	02:10	02:00	02:10	02:00	02:10	02:00
	Depth	0.36	0.36	0.35	0.36	0.35	0.35	0.35	0.35	0.35	0.35	0.35	0.35	0.35
Eendrachtstraat	Duration	02:15	02:10	02:05	02:10	02:00	02:10	02:00	02:10	02:00	02:10	02:00	02:10	02:00
	Depth	0.32	0.32	0.31	0.32	0.31	0.32	0.31	0.32	0.31	0.31	0.31	0.31	0.31

Table 11: Number of vulnerable buildings for all scenarios. The scenario with the least amount of vulnerable buildings is highlighted in blue.

Risk	Reference	L1-Ak-WP057	L1-Ag-WP057	L1-Ak-WP080	L1-Ag-WP080	L2-Ak-WP057	L2-Ag-WP057	L2-Ak-WP080	L2-Ag-WP080	L3-Ak-WP057	L3-Ag-WP057	L3-Ak-WP080	L3-Ag-WP080
Total	948	943	935	942	937	938	937	939	937	936	929	937	930
Low	610	606	605	607	607	606	607	605	607	606	602	606	602
Mid	209	209	202	207	201	203	201	205	201	202	200	202	201
High	129	128	128	128	129	129	129	129	129	129	127	129	127

Interestingly, the total difference in stored volume does not increase together with the total amount of added storage per scenario, which is shown in Figure 20. Instead, the difference in stored volume consistently increases in the scenarios in which the water level is -0.80 m NAP. This is caused by the lower water level allowing for more water to be stored in the canal and Spoorsingel, as well as decreasing the discharge to other waterways. Additionally, the lower water level also increases the possibilities for groundwater storage. Lowering of the water level also has the side effect of decreasing the discharge to the sewage treatment plant by decreasing the amount of groundwater leaking into the sewerage system. This is due to the many leaking sewers located close to the Spoorsingel, where the water level is decreased the most. Inversely, implementing the canal with a water level of -0.57 m NAP increases the amount of groundwater leaking into sewers due to the increase in groundwater level and subsequent pressures (see Section 4.4.4).

Disconnecting of the Zeevaardersbuurt mostly has an influence on the discharge of sewage to the sewage treatment plant and to the Nieuwe Maas. The reason for this is the implementation of the rain water sewer, which relieves the pressure on the combined sewerage system during the rainfall peak. This also makes for a slight increase in the availability of storage space in the sewers.

Both large-scale disconnecting as well as lowering of the water level in the canal are amplified for an increasing length of the canal. On itself, the length of the canal does not have major influences on the water balance. Still, it can be seen that water balance terms are more equal between scenarios with L2 and L3 than for scenarios with L1 and L2. This is likely caused by the culvert connecting the canal to the Spoorsingel being short for L3, which leads to less impoundment and more

discharge from the canal into the Spoorsingel, from where water is then pumped towards the Oude Haven.

The results show that increasing the available storage space adds to the reduction of pluvial flooding, regardless of whether the storage is added in the form of a longer canal, a lower water level in the canal or installation of a rain water sewer. Yet, one should be careful with drawing conclusions and consider the results in their context. While disconnecting of the Zeevaardersbuurt does increase the total amount of water stored in the study area and decrease flood duration in the subsided areas west of the Binnensingel, it also causes longer flood durations in the Zeevaardersbuurt itself. To prevent this, the provided additional storage (in the form of a larger rain water sewer or more surface water) should be increased. Lowering of the water level in the canal does show a strong increase in the amount of water stored in the study area, but also implies a local lowering of the groundwater level. This is a high-risk and often ill-advised measure in areas where the soil is predominantly clay or peat, as lowering of the groundwater level will inevitably cause subsidence. Even in areas with soils that are less prone for subsidence, lowering the groundwater level decreases the robustness of the water system.
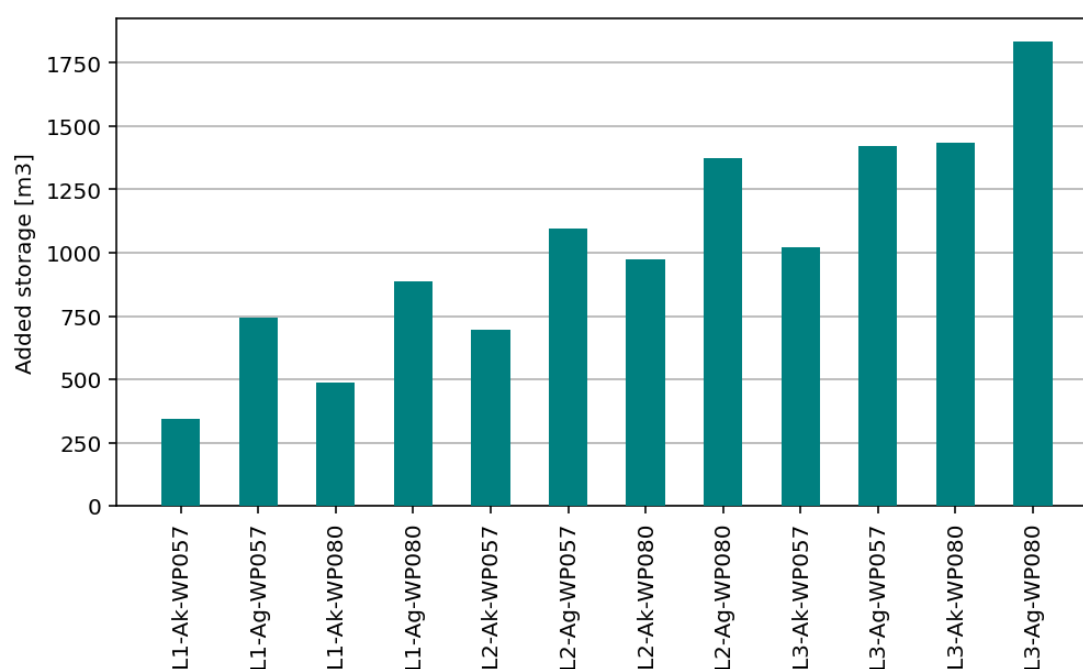
Figure 20: Storage added to the study area per scenario. It is assumed that disconnecting of the Zeevaardersbuurt adds 400 m³ of storage.

Table 12: Average water balance volumes for all measure variants. Absolute volumes are given in m^3. Optimal values are indicated in blue.

Scenario	Total Δ stored	Δ sewerage storage	Δ surface water storage	Δ groundwater storage	Total discharged	To sewage treatment plant	To Nieuwe Maas	To other waterways
Reference abs.	16716	1485	6471	8761	31089	13808	8493	8788
Reference rel.	35.0%	3.1%	13.5%	18.3%	65.0%	28.9%	17.8%	18.4%
L1-Ak-WP057	0.1pp	0.1pp	-0.6pp	0.7pp	-0.1pp	0.1pp	-0.3pp	0.0pp
L1-Ag-WP057	0.7pp	0.1pp	0.0pp	0.8pp	-0.8pp	-0.2pp	-1.2pp	0.5pp
L1-Ak-WP080	2.2pp	0.1pp	0.5pp	1.7pp	-2.3pp	-0.2pp	-0.4pp	-1.7pp
L1-Ag-WP080	2.0pp	0.1pp	0.2pp	1.8pp	-2.0pp	-0.5pp	-1.3pp	-0.4pp
L2-Ak-WP057	0.1pp	0.1pp	-0.3pp	0.4pp	-0.2pp	0.1pp	-0.4pp	0.0pp
L2-Ag-WP057	0.7pp	0.1pp	0.2pp	0.5pp	-0.8pp	-0.2pp	-1.3pp	0.6pp
L2-Ak-WP080	2.4pp	0.1pp	0.8pp	1.6pp	-2.3pp	-0.3pp	-0.4pp	-1.7pp
L2-Ag-WP080	3.1pp	0.1pp	1.4pp	1.7pp	-3.1pp	-0.5pp	-1.3pp	-1.3pp
L3-Ak-WP057	0.3pp	0.0pp	-0.2pp	0.5pp	-0.3pp	0.0pp	-0.5pp	0.1pp
L3-Ag-WP057	0.4pp	0.2pp	-0.2pp	0.5pp	-0.4pp	-0.4pp	-1.4pp	1.3pp
L3-Ak-WP080	2.5pp	0.1pp	1.1pp	1.4pp	-2.5pp	-0.3pp	-0.6pp	-1.8pp
L3-Ag-WP080	3.1pp	0.2pp	1.5pp	1.5pp	-3.1pp	-0.6pp	-1.4pp	-1.2pp

4.4.4 Groundwater table

For the scenarios with the full-lenght canal, the difference between the newly generated rasters and the original initial groundwater levels raster is shown in Figure 21. For a water level of -0.57 m NAP in the canal, little changes in the groundwater level along the Spoorsingel and the south of the canal, as the current water level (and thus surrounding groundwater levels) at this location is already at -0.57 m NAP. Further north around the canal, groundwater levels are raised by up to 40 cm. The extent to which the groundwater levels change is approximately 100 meters from the canal. For the water level of -0.80 m NAP, differences along the canal are less drastic, as the water level of -0.80 m was chosen due to it being close to the long-term average groundwater level. Along the south, a decrease of 20 to 30 cm is visible, which is to be expected due to the decrease of the water level in the Spoorsingel.

4.4.5 Groundwater fluctuations

Figure 22 shows the standard deviation in the groundwater level over the simulation time for the most extreme scenario (L3-Ag-WP080). It can be seen that compared to the reference situation, the groundwater fluctuations have decreased at the location of the canal. However, this is highly local and only has an effect up to 20 m from the canal. The only place outside of the Binnensingel where a change is visible, is the pond in the Oranjepark to which the canal is connected. Compared to the reference situation, the standard deviation here has slightly risen due to the additional inflow.

In the Zeevaardersbuurt, the standard deviation has increased around the Nieuwe Kerkstraat. This is only present in the scenarios where the Zeevaardersbuurt is disconnected and the water level in the canal is -0.80m, and to a smaller extent when the water level is -0.57 m. In the scenarios where the Zeevaardersbuurt is not disconnected and the water level is -0.57m, the standard deviation does not change from the reference situation. This is likely caused by the Nieuwe Kerkstraat being flooded for a longer duration in the reference situation than in the scenarios in which it is disconnected (as explained in Section 4.4.1).
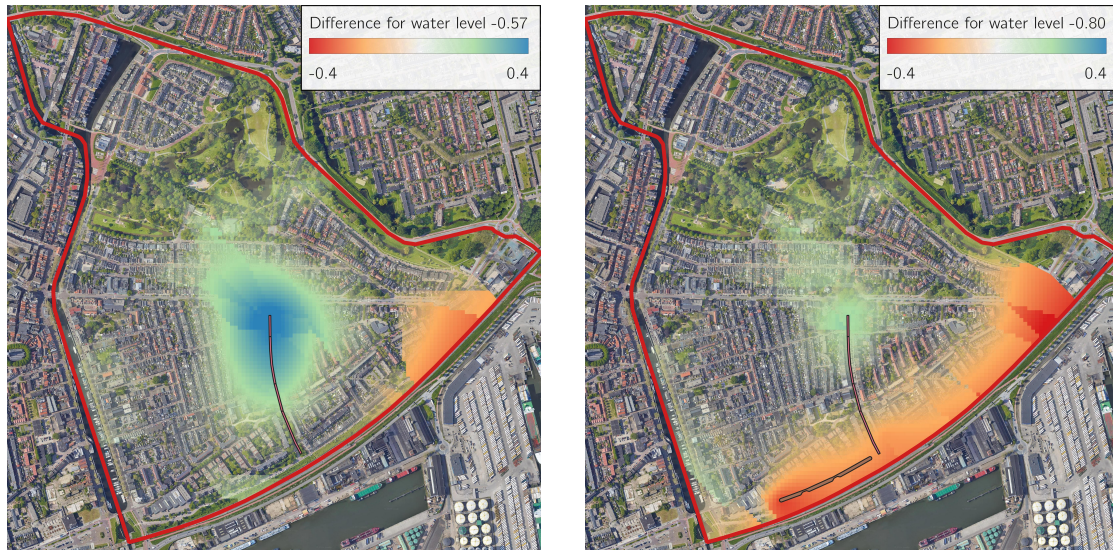
Figure 21: Maps showing the difference in the initial groundwater level used by the model when the initial groundwater level raster for the reference situation is substracted from a revised one (for the full-length canal, as depicted in the image). Blue thus indicates a rise of the groundwater level, while red indicates lowering of the groundwater level. Neutral values, indicating no or little change, have been made transparent.
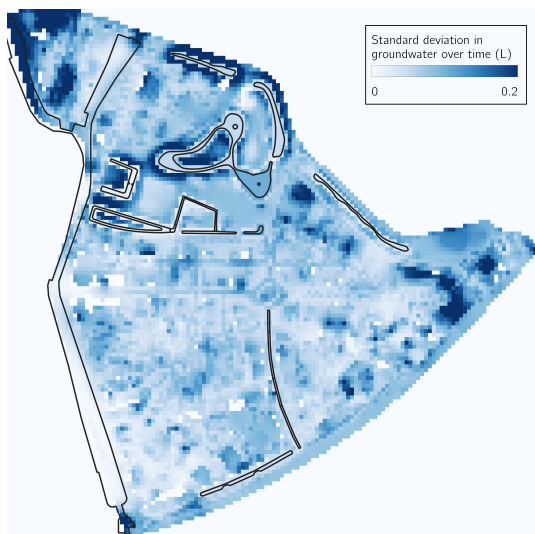
Figure 22: Raster showing the standard deviation in the groundwater level over time for every grid cell for scenario L3-Ag-WP080. Note the addition of the canal on the Binnensingel.
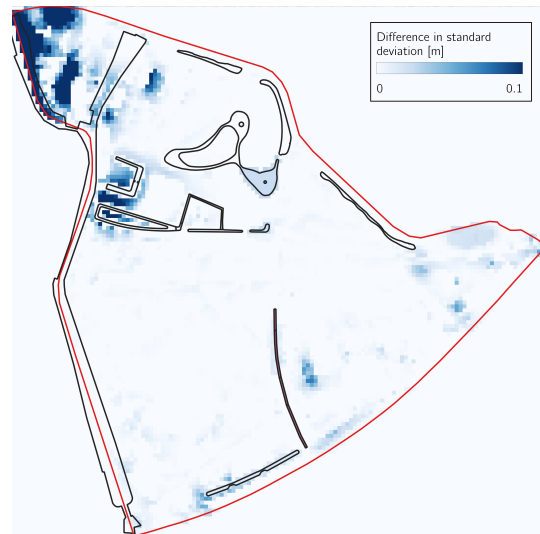
Figure 23: Raster showing the differences in the standard deviation in the groundwater level over time for every grid cell between scenario L3-Ag-WP080 and the reference scenario (current situation). The red line outlines the study area.

5 Discussion

5.1 Limitations

5.1.1 Groundwater model

This study is the first in which the groundwater module of 3Di has been extensively used in an urban context. Despite being simplified to a relatively large extent, the groundwater module has proven to be able to accurately simulate groundwater levels and to work very well as part of a wider integral model. The module does however show more potential than what was used in this study, partly because of time constraints and partly because of a lack of experience with practical use of this module. The following paragraphs elaborate on this.

Computational grid In the schematisation as provided by Nelen & Schuurmans, buildings were cut from the DEM as a method to prevent virtual overland flow through buildings. At several locations, this resulted in an incomplete computational grid with missing computational cells or flowlines. As the groundwater domain and the surface domain are equal, this effectively means that groundwater cannot flow underneath buildings.

The extent to which this makes for an unrealistic schematisation of reality can be discussed and differs per case. If many large underground structures, like cellars, are present, (partial) blockage of groundwater flow can be assumed. For the Oostwijk, the number of cellars is unknown.

A possible alternative method would be to increase the DEM-values at the locations of buildings, which prevents flow through buildings, combined with the addition of an interception raster, which prevents rain falling on buildings to be added to the model twice. This method leaves the DEM and the computational grids intact. In tests, this method results in the groundwater level dropping by 10-20 cm compared to the method used in this study (see Figure 24). While this particular example is from the middle of the study area, it is found that the difference between the two methods is relatively constant over most of the study area. As the study is interested more in groundwater fluctuations rather than absolute groundwater levels, it is expected that this modelling flaw does not have a major impact on the results regarding groundwater fluctuations as presented by the study. Still, the overestimation of groundwater levels does potentially cause an overestimation of flood durations in heavily subsided areas, although the extent of this is unknown.

Nevertheless, applying the interception method is strongly suggested for future groundwater studies.
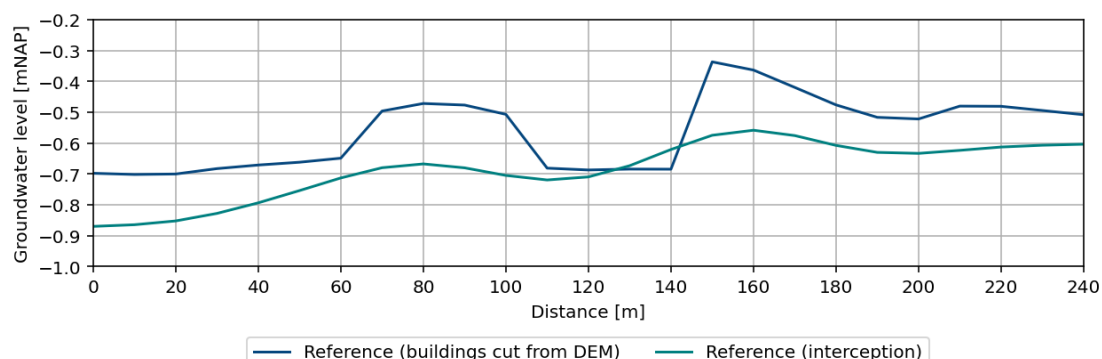
Figure 24: Comparison between the calculated groundwater levels with buildings cut from the DEM and an intact DEM with an interception raster. The Binnensingel lies at Distance 125.

Boundaries No specific boundary conditions are set for the groundwater model. This is possible due to groundwater levels only sloping very slightly, meaning that there is relatively little exchange with groundwater oustide of the model domain. Additionally, the Oostwijk is surrounded by water features in the west, north and east, all of which are present in the model and thus already act as groundwater forcings along the majority of the models boundary.

While this makes for a realistic schematisation of reality at the western and nothern boundaries, this is not the case along the eastern model boundary. The area located east of the Oostwijk has a significantly lower surface elevation and consequently, the groundwater level below this area is on average two meters deeper than the groundwater in the Oostwijk. This makes that the groundwater in the Oostwijk is slowly drained to the east during times of drought, which is visible at the groundwater level measuring location at the Hogelaan during June 9-17th 2023 (see Figure 25). The figure also shows that in the schematisation, the groundwater level is forced upwards, which is caused by the nearby pond along the Parkweg.

To implement the draining effect of the neighbouring area, a boundary condition should be implemented along the eastern boundary of the Oostwijk. While tried, the study did not manage to do so successfully within the given time frame. It must therefore be noted that groundwater levels on the eastern side of the Oostwijk are getting increasingly overestimated by the model the longer the simulated weather is dry.
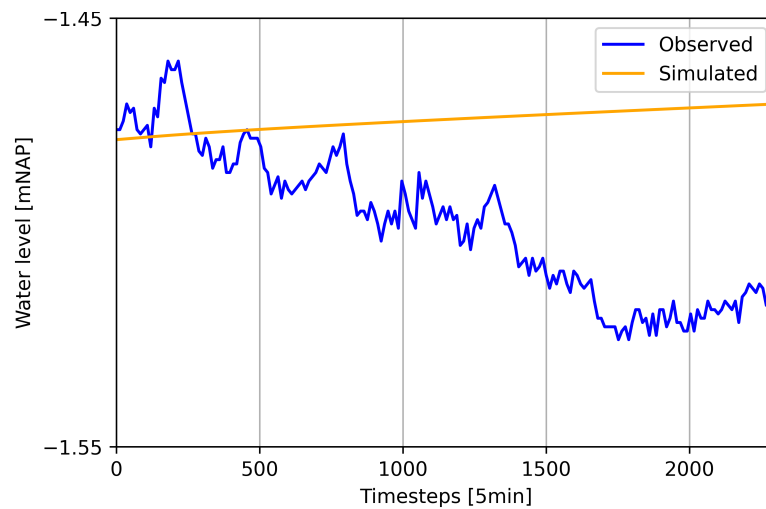
Figure 25: Observed and simulated groundwater level at the Hogelaan during June 9-17th 2023. The simulated groundwater level is made with the calibrated model.

Simplification   In general, the groundwater model is heavily simplified. Constant parameter values for hydraulic conductivity and porosity were chosen while the soil in the urban environment is highly heterogeneous. Although the most of these variations cannot be accounted for due to (1) the small physical scale of these variations and (2) a lack of data, consistent variations from the natural environment, for example the sandy layers underneath roads and around sewers, could be implemented into the model with relative ease. This would allow for a more accurate schematisation of the exchange process between groundwater and leaking sewers.

Interpolation   These varying soil types, together with sewers, irregular infiltration possibilities or blockages such as cellars also cause the groundwater levels in urban areas to show large differences over short distances. These irregularities have not been taken into account into the interpolation of initial water levels, as this would require data from an unrealistically dense groundwater measuring network. Still, the groundwater level interpolation could be improved by placing virtual groundwater level forcing on surface waters. The interpolation could be further improved by using the average groundwater levels over summer as input instead of the average groundwater level over the entire year. This would make for a more realistic simulation, considering the intensity of the used composite rainfall event and the KNMI forecasting the heaviest increase in rain intensity in summer (KNMI, 2023). However, both changes are expected to be of little importance to the results due to the scope of the study. Detailing the interpolation would mainly influence the initial groundwater level raster in the Oranjepark, while the results focus on the

south of the Oostwijk where surface water is scarce, and although using only input from summer would change the absolute groundwater values, the study is mainly interested in groundwater fluctuations.

Leakage   The initial value for the leakage parameter is taken from a study done on the island of Texel (Kling, 2019). Although the leakage direction is equal in both cases, the soil conditions on Texel are the inverse of the conditions in the Oostwijk: on Texel, a 10 m thick sandy layer lies on top of a badly permeable clay layer. Adopting the leakage factor for the Oostwijk from Texel is therefore done under the assumption that the influence of leakage is so small that variations in its magnitude do not affect the results of the study. This assumption is confirmed in the sensitivity analysis, where the KGE of the model results does not visibly change for different values of leakage (see Figure 11).

5.1.2   Vulnerable buildings

Vulnerable buildings are derived by creating a buffer with a width of 0.5 m around each building. The median surface level within this buffer is used as the floor level of the building, to which the water level is subsequently compared to determine the risk extent of said building. For the row of buildings next to the Oude Haven, the surface elevation along the back facades is 1 to 1.5 m lower than the elevation at the front facade. Due to this discrepancy, the determined floor level lies somewhere in between the two surface elevations. Although ponding at the front facades is very limited, the resulting water level is still significantly higher than the used floor level, which causes the entire row of buildings to be classified as high-risk. In reality, only the buildings with significant ponding against the front and/or back facades are considered high-risk. To assess this more accurately, the floor level of the front and back facades should be determined separately. Due to the flat nature of the Oostwijk, this methodological flaw has not had further influence on the classification of vulnerable buildings.

5.1.3   Used rainfall event

The results show only very small differences between scenarios in both pluvial flooding and groundwater fluctuations. Although these results already show the potential of the addition of a canal to the study area, the quantified effects could have been influenced by the used methods. For pluvial flooding, the effect of the measures could have been larger if a less intense rainfall event was used. The future rainfall event used in the study is a very intense event compared to the conditions for which the current sewerage system in the study area is designed, which causes a

lot of pluvial flooding. A relatively small intervention like the addition of a canal is therefore unlikely to have a large effect. To put this into perspective: the full-length canal adds an area of 1800 m^2 to the existing 26600 m^2 of surface water in the Oostwijk, which is an increase of only 7%. The canal could potentially have a bigger effect during a less intense rainfall event that would only cause mild pluvial flooding. Evaluating a wider range of rainfall events would therefore give a more detailed quantification of the effects of the canal and thus be more relevant for policy makers. It must be noted however that the chosen future rainfall event is no fictional event and is likely to become more common in the future. Still, the relevance of the results of the study depend on the accepted frequency and extent of pluvial flooding by policy makers.

Regarding groundwater, the study would have benefitted from working with a longer simulation time. Although groundwater flows in the study area are relatively rapid and groundwater levels have moved to a tranquil state within a simulation time of a week, the simulation of a sequence of rainfall events with intermittent dry periods in particular would give much more insight in groundwater fluctuations. This does come at the cost of longer computational times, which were not available in this study. Still, the results of the study can be interpreted as a quick-scan on groundwater fluctuations in the study area.

5.2   Generalisation

The Oostwijk is, with its dense housing and a very high amount of impervious area, typical for many neighbourhoods in cities in the western part of the Netherlands. Results of the study are therefore likely applicable to more cities in this area. Additionally, effects will be comparable in other areas with clayey soils, such as Flevoland.

On an international scale, large urban areas in subsiding deltas are present mostly in south-east Asia. Notable examples of these 'sinking cities' are Bangkok, Jakarta and Dhaka (Deltares, 2015). Although the soil conditions may be similar to the conditions in the Oostwijk, these Asian cities themselves are even more densely populated and exist of significantly more high-rise buildings than the Oostwijk. The extreme weight exerted on the soil by these buildings and large groundwater depletions to satisfy drinking water demand are the primary reasons for soil subsidence in the south-Asian cities (Erkens et al., 2015; Schmidt, 2015). Furthermore, rainfall conditions in south-east Asia differ significantly from the (future) rainfall conditions in the Netherlands. Due to these different circumstances, the results of this study are not directly applicable to other subsiding deltas. Still, the notion

that disconnecting towards a canal is a more efficient measure than increasing the length of the canal is expected to hold under different circumstances, as well as the fact that the implemented measures should be well-dimensioned to show their effect.

6 Conclusions and recommendations

6.1 Conclusions

The aim of this study was to quantify the effect of surface water as a climate adaptation measure by looking at pluvial flooding and groundwater fluctuations. To achieve this aim, an integrated hydrodynamic model containing surface water, surface runoff, sewerage and groundwater was calibrated and subsequently used to study the effects of the addition of a canal to the Oostwijk neighbourhood in Vlaardingen.

Calibration of the model mostly focussed on the groundwater component, which was added to the model. Based on a sensitivity analysis, the porosity, hydraulic conductivity and initial infiltration were found to be the most influential parameters on the accuracy of the groundwater model. These parameters, together with a parameter that correctly simulates exchanges between groundwater and leaking sewers, were used to calibrate the model. After calibration, the model could recreate historical groundwater levels with an accuracy with a KGE of 0.58 and MAE of 0.04 m, which was deemed to be sufficient. Although not well quantifiable, the sewerage model was qualitatively found to have sufficient accuracy.

To study the effect of a future rainfall event on the study area, a composite rainfall event with a recurrance time of 2 years, aduration of 10 hours, a cumulative volume of 43.5 mm and five-minute-peak intensity of 89 mm/h was chosen, which is compliant with the KNMI climate prediction for 2050. The rainfall event was followed by a week with no rain to allow the groundwater to stabilise. Applying this entire event on the model of the study area resulted in heavy pluvial flooding. In the subsided areas, standing water with a maximum depth of 25-30 cm was calculated for a duration of more than two hours. In the entire study area, 948 buildings were at risk of flooding. Over the simulation time, groundwater levels fluctuated up to 10 cm in mostly impervious areas and up to 30 cm in pervious areas next to ponds. Approximately 35% of all rainwater was stored in the study area, while 65% was discharged via sewers or surface water.

Implementation of the canal was done in scenarios where the length and water level of the canal and the size of disconnected area used as inflow for the canal were varied. The results showed that creating storage, either through a longer canal, a lower water level in the canal or a larger disconnected area, resulted in less pluvial flooding. Still, the reductions were small, with up to 2 cm in depth,

15 minutes in duration and 19 vulnerable buildings. Groundwater level fluctuations were decreased only locally (up to 20 m) around the canal. The implemented measures caused the amount of water stored in the study area to increase by a maximum of 3%.

6.2 Recommendations for municipality

If the municipality of Vlaardingen does not want to widen its acceptance of flooding as a result of a precipitation event with a return period of 2 years, the study shows that action must be taken in the Oostwijk. Although the results of the study only show a small decrease in pluvial flooding due to implementation of the proposed measures, the results are still promising. Disconnecting has shown to have a strong reducing effect on the duration and depth of pluvial flooding when applied in combination with a canal. This is despite the study mostly focussing on the Zeevaardersbuurt, in which pluvial flooding problems are too large to solve with disconnecting only. It is therefore recommended to investigate the possibilities of disconnecting in the part of the Oostwijk west of Binnensingel, where streets are also subsided and subject to pluvial flooding. These problems are however on a lesser scale than the problems in the Zeevaardersbuurt and disconnecting in combination with a canal on the Binnensingel does therefore have a larger problem-solving potential for this area.

It is also recommended to investigate the lowering of the (ground)water level. In consultation with the municipality it was found that most of the soil layers that were susceptible to subsidence are almost fully subsided, so lowering of the groundwater level would be unlikely to cause more subsidence. Still, research must be done on the influence of eventual groundwater lowering during the winter period and on the influences on drought, foundations and (albeit) sparce vegetation.

Additionally, it is recommended to investigate the effect that replacement of leaking sewers has on groundwater levels, which will rise when the draining effect of leaking sewers is removed. This could potentially lead to groundwater hindrance in subsided areas and thus require the installation of more drainage pumps.

6.3 Recommendations for future research

For similar future research it is recommended to use a sequence of dry periods and rainfall events, which have different lengths and return periods. By simulating events with a variety of return periods, a better insight into the effects of a

climate-adaptive measure can be achieved. This is expected to be particularly useful for shorter return times, such as 1 and 0.5 years. Simulating a longer sequence also gives more insight in groundwater fluctuations. Additionally, when using the 3Di hydrodynamic software, it is recommended to avoid cutting buildings from the DEM when working with groundwater. Instead, the DEM should be heightened at the locations of buildings and an interception raster should be applied to prevent 'double rain' input. This method keeps the computational grid intact and allows groundwater to flow beneath buildings at all times.

This research has added to literature by integrally studying the effects of open water in an urban area with high groundwater levels on pluvial flooding and groundwater fluctuations. It has however done so for a future summer rainfall event. It is however still unknown how open water can attribute to a healthy urban water system in times of drought, specifically by regulating the groundwater table. Therefore, it is recommended to study the interaction between urban open water and groundwater in times of drought.

Additionally, this study has shown that the flow routing towards open water is an important aspect in the effectiveness urban open water has on reducing pluvial flooding. Due to spatial limitations in an urban context, it is not always feasible to implement open water at the naturally best location (i.e. the location with the lowest surface elevation). It is therefore useful to study the options for rainwater routing, both on surface level as well as underground.

References

3diwatermanagement.com. (2024). About us. https://3diwatermanagement.com/about-us/ [Online, accessed April 12, 2024].

Ariza, S. L. J., Martínez, J. A., Muñoz, A. F., Quijano, J. P., Rodríguez, J. P., Camacho, L. A., & Díaz-Granados, M. (2019). A multicriteria planning framework to locate and select sustainable urban drainage systems (suds) in consolidated urban areas. *Sustainability*, *11*(8). https://doi.org/10.3390/su11082312

Borden, R. C. (2006). Protocol for enhanced in situ bioremediation using emulsified edible oil.

Bot, B. (2011). Grondwaterzakboekje.

Brown, S., & Nicholls, R. (2015). Subsidence and human influences in mega deltas: The case of the ganges-brahmaputra-meghna. *Science of The Total Environment*, *527*, 362–374. https://doi.org/10.1016/j.scitotenv.2015.04.124

Carmen, N. B., Hunt, W. F., & Anderson, A. R. (2016). Volume reduction provided by eight residential disconnected downspouts in durham, north carolina. *Journal of Environmental Engineering*, *142*(10). https://doi.org/10.1061/(ASCE)EE.1943-7870.0001107

CBS. (2024). Kerncijfers wijken en buurten 2023. https://www.cbs.nl/nl-nl/maatwerk/2024/11/kerncijfers-wijken-en-buurten-2023 [Online, accessed June 26, 2024].

Clark, M. P., Vogel, R. M., Lamontagne, J. R., Mizukami, N., Knoben, W., Tang, G., Gharari, S., Freer, J. E., Whitfield, P. H., Shook, K. R., & Papalexiou, S. M. (2021). The abuse of popular performance metrics in hydrologic modelling. *Water Resources Research*, *57*. https://doi.org/10.1029/2020WR029001

de Jong, S. P., Oosthof, J., Kluck, Tjallingii, S. P., & Blom, G. E. (2001). *Afkoppelen in delfland en schieland*. Tauw.

Deltares. (2015). Sinking cities. https://cms.deltares.nl/assets/common/downloads/Sinking-cities-1.pdf [Online, accessed January 27, 2025].

DGBC. (2023). *Framework for climate adaptive buildings - standaard-aanpak voor het inschatten van fysieke klimaatrisico's voor bestaande gebouwen, deel 2: De gebouwscore*. https://www.dgbc.nl/publicaties/framework-climate-adaptive-buildings-63

DINOloket. (2024). Ondergrondgegevens. https://www.dinoloket.nl/ondergrondgegevens [Online, accessed May 29, 2024].

Dupuit, J. (1863). Etudes théoriques et pratiques sur le mouvement des eaux dans les canaux découverts et à travers les terrains perméables. *Dunod*, *2*.

Eigenhuijsen, E., Wentink, R., & van Oosterwijk, H. (2009). *Handreiking afkoppelen: Afkoppelen in de provincie limburg*. Tauw.

el Kajjal, S., & Mogos, B. (2021). *Basisrioleringsplan ++*. Witteveen+Bos.

Erkens, G., Bucx, T., Dam, R., Lange, G. D., & Lambert, J. (2015). Sinking coastal cities. *Proc. IAHS*, *372*, 189–198. https://doi.org/10.5194/piahs-372-189-2015

Fletcher, B. C. (2009). *Downspout disconnection suitability and incentives analysis*.

Gan, T., Dlamini, E., & Biftu, G. (1997). Effects of model complexity and structure, data quality and objective functions on hydrologic modeling. *Journal of Hydrology*, *192*(1-4), 81–103. https://doi.org/10.1016/S0022-1694(96)03114-9

Gilliom, R., Bell, C. D., Hogue, T. S., & Mccray, J. E. (2019). A rainwater harvesting accounting tool for water supply availability in colorado. *Water*, *11*(11). https://doi.org/10.3390/w11112205

Gorelick, S., & Zheng, C. (2015). Global change and the groundwater management challenge. *Water Resources Research*, *51*(5), 3031–3051. https://doi.org/10.1002/2014WR016825

Guo, K., Guan, M., & Yu, D. (2021). Urban surface water flood modelling – a comprehensive review of current models and future challenges. *Hydrology and Earth System Sciences*, *25*(5), 2843–2860. https://doi.org/10.5194/hess-25-2843-2021

Gupta, H. V., & Kling, H. (2011). On typical range, sensitivity, and normalization of mean squared error and nash-suthcliffe efficiency type metrics. *Water Resources Research*, *47*(10). https://doi.org/https://doi.org/10.1029/2011WR010962

Hoogheemraadschap van Delfland. (2024). Het juiste waterpeil. https://hhdelfland.maps.arcgis.com/apps/instant/sidebar/index.htmlappid=b464f815c0af48178bdef923c11373e [Online, accessed June 20, 2024].

Horton, R. E. (1933). The role of infiltration in the hydrologic cycle. *Transactions, American Geophysical Journal*, *14*, 446–460.

Imran, H., Akib, S., & Karim, M. (2013). Permeable pavement and stormwater management systems: A review. *Environmental Technology*, *34*(18). https://doi.org/10.1080/09593330.2013.782573

IPCC. (2023). *Climate change 2023: Synthesis report. contribution of working groups i, ii and iii to the sixth assessment report of the intergovernmental panel on climate change*. https://www.ipcc.ch/report/ar6/syr/

Jandaghian, Z., & Colombo, A. (2024). The role of water bodies in climate regulation: Insights from recent studies on urban heat island mitigation. *Buildings*, *24*(9). https://doi.org/10.3390/buildings14092945

Joostdevree.nl. (2024). K-waarde. https://www.joostdevree.nl/shtmls/k-waarde. shtml [Online, accessed May 29, 2024].

Kim, J.-W., Lu, Z., Jia, Y., & Shum, C. (2015). Ground subsidence in tucson, arizona, monitored by time-series analysis using multi-sensor insar datasets from 1993 to 2011. *Journal of Photogrammetry and Remote Sensing*, *107*, 126–141. https://doi.org/10.1016/j.isprsjprs.2015.03.013

Klemes, V. (1986). Operational testing of hydrological simulation models. *Hydrological Sciences Journal*, *31*(1), 13–24. https://doi.org/10.1080/02626668609491024

Kling, D. J. (2019). *Application and evaluation of the 3di groundwater model in the waalenburg polder, texel, the netherlands.*

KNMI. (2014). *Knmi'14: Climate change scenarios for the 21st century – a netherlands perspective* (WR 2014-01).

KNMI. (2023). *Knmi'23 - klimaatschenarios voor nederland* (No. 23-03).

Knoben, W. J. M., Freer, J. E., & Woods, R. A. (2019). Technical note: Inherent benchmark or not? comparing nash-sutcliffe and kling-gupta effiency scores. *Hydrology and Earth System Sciences*, *23*(10). https://doi.org/10.5194/hess-23-4323-2019

LBn betonproducten. (2010). Productoverzicht riolering. https://www.lbn.nu/resources/site1/General/Productoverzicht_LBN_2016.pdf [Online, accessed June 25, 2024].

McGranahan, G., Balk, D., & Anderson, B. (2007). The rising tide: Assessing the risks of climate change and human settlements in low elevation coastal zones. *Environment & Urbanization*, *19*(1). https://doi.org/10.1177/0956247807076960

Melville-Shreeve, P., Cotterill, S., Grant, L., Arahuetes, A., Stovin, V., Farmani, R., & Butler, D. (2017). State of suds delivery in the united kingdom. *Water and Environment Journal*, *32*, 9–16. https://doi.org/10.1111/wej.12283

Merga, B. B., Tabor, K. W., & Melka, G. A. (2024). Analysis of the cooling effects of urban green spaces in mitigating micro-climate change using geospatial techniques in adama city, ethiopia. *Sustainable Environment*, *10*(1). https://doi.org/10.1080/27658511.2024.2350806

Munisense. (2024). Opendata.munisense.net. https://opendata.munisense.net/ [Online, accessed April 22, 2024].

Nelen & Schuurmans. (2024a). 2d groundwater flow. https://docs.3di.live/h_groundwater.html [Online, accessed April 23, 2024].

Nelen & Schuurmans. (2024b). Computational grid. https://docs.3di.live/h_computational_grid.html [Online, accessed January 3, 2025].

Neumann, B., Vafeidis, A., Zimmerman, J., & Nicholls, R. (2015). Futute coastal population growth and exposure to sea-level rise and coastal flooding - a global assessment. *PLOS ONE*, *10*(6). https://doi.org/10.1371/journal.pone.0131375

NIOO-KNAW. (2022). *De toestand van kleine wateren* (No. 260-71009). https://natuurenmilieu.nl/app/uploads/20221611-Rapportage-Watermonsters-2022-NIOO-KNAW.pdf

Patra, J., Kumar, R., & Mani, P. (2016). Combined fluvial and pluvial flood inundation modelling for a project site. *Procedia Technology*, *24*, 93–100. https://doi.org/10.1016/j.protcy.2016.05.014

RIONED. (2014). *Ervaringen met de aanpak van regenwateroverlast in bebouwd gebied*.

RIONED. (2019a). Bui01 - bui10. https://www.riool.net/bui01-bui10 [Online, accessed February 27, 2024].

RIONED. (2019b). Huishoudelijke afvoerwater. https://www.riool.net/kennisbank/onderzoek/modelleren-hydraulisch-functioneren/stap-iv-hydraulische-belasting-bepalen/droogweerafvoer-dwa/huishoudelijk-afvalwater [Online, accessed September 16, 2024].

RIONED. (2020). Composietbuien voor klimaatscenario's. https://www.riool.net/composietbuien-voor-klimaatscenario-s [Online, accessed March 4, 2024].

Sajib, A. M., Diganta, M., Moniruzzaman, M., Rahman, A., T, D., Uddin, M., & Olbert, A. I. (2024). Assessing water quality of an ecologically critical urban canal incorporating machine learning approaches. *Ecological Informations*, *80*. https://doi.org/10.1016/j.ecoinf.2024.102514

Schets, F. M., van Wijen, J. H., Schijven, J. F., Schoon, H., & de Rode Husman, A. M. (2008). Monitoring of waterborne pathogens in surface waters in amsterdam, the netherlands, and the potential health risk associated with exposure to cryptosporidium and giardia in these waters. *Applied and Environmental Microbiology*, *74*(7). https://doi.org/10.1128/AEM.01609-07

Schmidt, C. (2015). Delta subsidence: An imminent threat to coastal populations. *Environmental Health Perspectives*, *123*(8), 204–209. https://doi.org/10.1289/ehp.123-A204

Sman, H. (2015). *Grondwatermodellering a4 delft - schiedam*. Deltares.

Steenbergen, A. (2008). *Hoe gemeenten om kunnen gaan met extreme regenval in de stad*.

Steeneveld, G., Koopmans, S., Heusinkveld, B., & Theeuwes, N. (2014). Refreshing the role of open water surfaces on mitigating the maximum urban heat island effect. *Landscaping and Urban Planning*, *121*, 92–96. https://doi.org/10.1016/j.landurbplan.2013.09.001

Stoorvogel, J., Bakkenes, M., Temme, A., Batjes, N., & ten Brink, B. (2016). S-world: A global soil map for environmental modelling. *Land Degradation & Development*, *28*(1), 22–33. https://doi.org/10.1002/ldr.2656

STOWA. (2009). *Water terug in de stad* (No. 5). https://www.stowa.nl/sites/default/files/assets/PUBLICATIES/Publicaties%202000-2010/Publicaties%202005-2009/STOWA%202009-05.pdf [Online, accessed January 20, 2025].

STOWA. (2017). *Benchmark inundatiemodellen*.

STOWA. (2019a). *Afkoppelen: Kansen en risico's van anders omgaan met hemelwater in de stad* (No. 22).

STOWA. (2019b). *Neerslagstatistiek en -reeksen voor het waterbeheer 2019* (No. 19).

STOWA. (2023). *Beoordeling neerslagstatistiek: Meteo-onderzoek ten behoeve van het waterbeheer: Deelrapport 1* (No. 35).

USACE. (2024). Hec-ras 2d user manual: Infiltration methods. https://www.hec.usace.army.mil/confluence/rasdocs/r2dum/latest/developing-a-terrain-model-and-geospatial-layers/infiltration-methods [Online, accessed September 23, 2024].

Vaes, G., & Berlamont, J. (1996). Composietbuien als neerslaginvoet voor rioleringsberekeningen.

van Baaren, E., Bootsma, H., & Essink, G. O. (2018). *Referentiesituatie hydro(geo)logie zuid-holland*. COASTAR.

van Dorland, R., Beersma, J., Bessembinder, J., Bloemendaal, N., van den Brink, H., Blanes, M. B., Drijfhout, S., Groenland, R., Haarsma, R., Homan, C., Keizer, I., Krikken, F., Bars, D. L., Lenderink, G., van Meijgaard, E., Meirink, J. F., Overbeek, B., Reerink, T., Selten, F., . . . van der Wiel, K. (2024). *Knmi national climate scenarios 2023 for the netherlands* (WR-23-02).

Vasenev, V. I., Stoorvogel, J. J., & Vasenev, I. I. (2013). Urban soil organic carbon and its spatial heterogeneity in comparison with natural and agricultural areas in the moscow region. *Catena*, *107*, 96–102. https://doi.org/10.1016/j.catena.2013.02.009

VMM. (1996). Bijlage c : Bijkomende informatie over grachten. https://www.vlario.be/files/bijlageC.pdf [Online, accessed January 20, 2025.

Volp, N. D., Prooijen, B. C. V., & Stelling, G. S. (2013). A finite volume approach for shallow water flow accounting for high-resolution bathymetry and roughness data. *Water Resources Research*, *49*, 4126–4135. https://doi.org/10.1002/wrcr.20324

Vozinaki, A., Morianou, G., Alexakis, D., & Tsanis, I. (2017). Comparing 1d and combined 1d/2d hydraulic simulations using high-resolution topographic

data: A case study of the koiliaris basin, greece. *Hydrological Sciences Journal*, *62*(4). https://doi.org/10.1080/02626667.2016.1255746

Wang, K., Onodera, S., Saito, M., & Shimizu, Y. (2021). Long-term variations in water balance by increase in percent imperviousness of urban regions. *Journal of Hydrology*, *602*. https://doi.org/10.1016/j.jhydrol.2021.126767

Wang, Y., Berardi, U., & Akbari, H. (2016). Comparing the effects of urban heat island mitigation strategies for toronto, canada. *Energy and Buildings*, *114*, 2–19. https://doi.org/10.1016/j.enbuild.2015.06.046

Wiebing, R. G. (2023). *Effectiveness of adaptation measures to make the urban rainwater distribution more robust after short intense rainfall events*.

Woessner, W., & Poeter, E. (2020). *Hydrogeologic properties of earth materials and principles of groundwater flow*. The Groundwater Project.

Zhan, Q., Teurlincx, S., van Herpen, F., Raman, N. V., Lürling, M., Waajen, G., & de Senerpont Domis, L. N. (2022). Towards climate-robust water quality management: Testing the efficacy of different eutrophication control measures during a heatwave in an urban canal. *Science of The Total Environment*, *828*. https://doi.org/10.1016/j.scitotenv.2022.154421

A Derivation of the start and stop levels of pumping station Boslaan

While the BRP (el Kajjal & Mogos, 2021) does not state specific start and stop levels, it does state that pumps 1 and 2 have the same specifications and that pump 3 is the spillway pump leading to the Nieuwe Maas. The start and stop levels of the pumps at pumping station Boslaan as originally present in the model do not match the information from the BRP. Pumps 1 and 2 have different start and stop levels, and pump 1 has a higher start level than pump 3, which would mean that the spillway would be used before the maximum DWA pumping capacity is reached. Together, this makes it very likely that the model will give unrealistic results if the start and stop levels are not adjusted.

By using the data on the water level in the sewers at pumping station Boslaan, an indication of the start and stop levels used in practice can be retrieved. The water level over the entirety of 2022 is plotted in Figure 26. In this graph, two clear horizontal lines can be plotted: one at -2.80 m and one at -3.25 m. This indicates that these levels are the respective start and stop level of pumps 1 and 2. The start and stop level of pump 3 are more difficult to define as this pump is in use less often. Still, the start and stop levels originally in the model perfectly complement the found start and stop levels op pump 1 and 2. It is therefore assumed that pump 3 has a start level of -1.57 m and a stop level of -2.80 m.

Table 13: Start and stop levels of the pumps at pumping station Boslaan.

Pump	Start level [mNAP]		Stop level [mNAP]	
	Original	Derived	Original	Derived
Boslaan 1	-0.50	-2.80	-1.00	-3.25
Boslaan 2	-2.40	-2.80	-3.10	-3.25
Boslaan 3	-1.57	-1.57	-2.80	-2.80
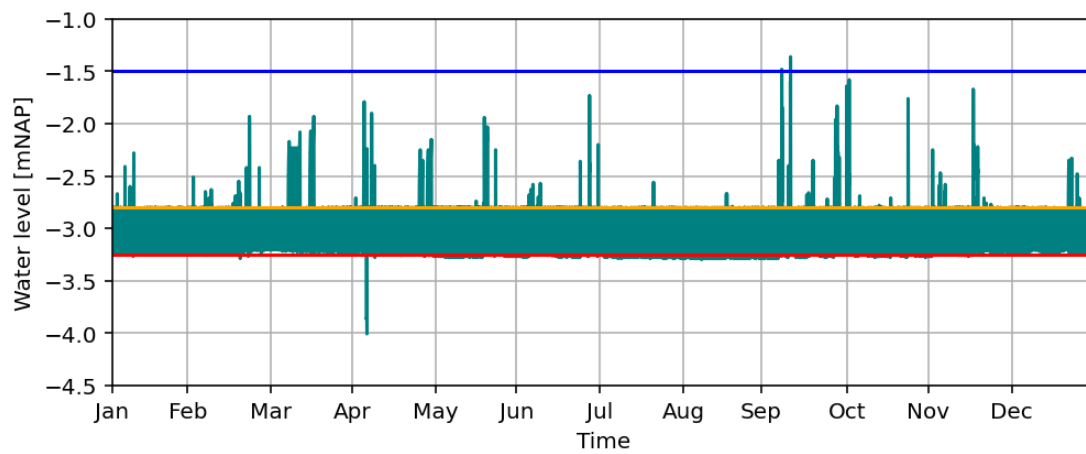
Figure 26: Plot of the water levels in the sewer at pumping station Boslaan over 2022. The blue line indicates the start level of the spillway pump, the orange line the stop level of the spillway pump and the start level of the regular pumps and the red line the stop level of the regular pumps.

B Observed vs simulated groundwater levels after calibration
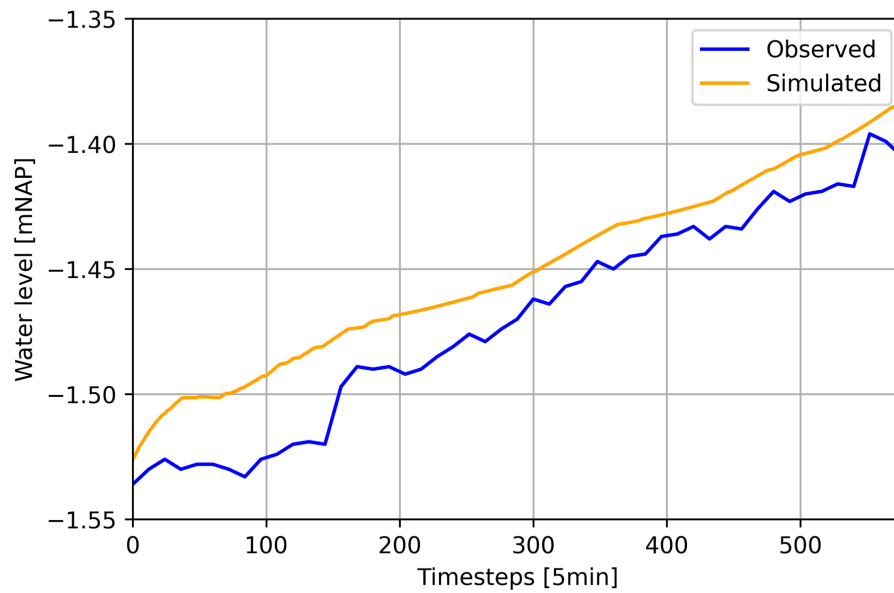
Figure 27: Groundwater levels at the Callenburgstraat during 12 and 13 October 2023.
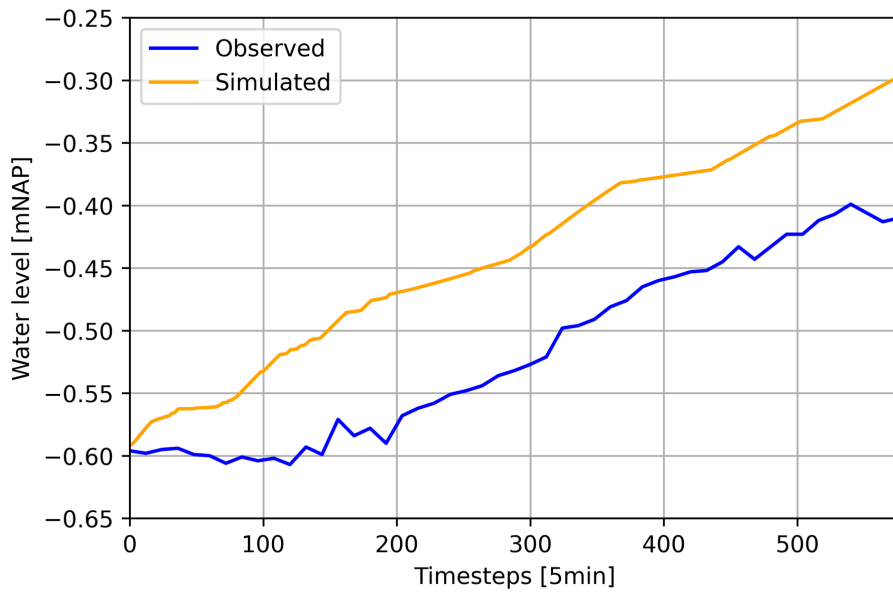
Figure 28: Groundwater levels at the Emmastraat during 12 and 13 October 2023.
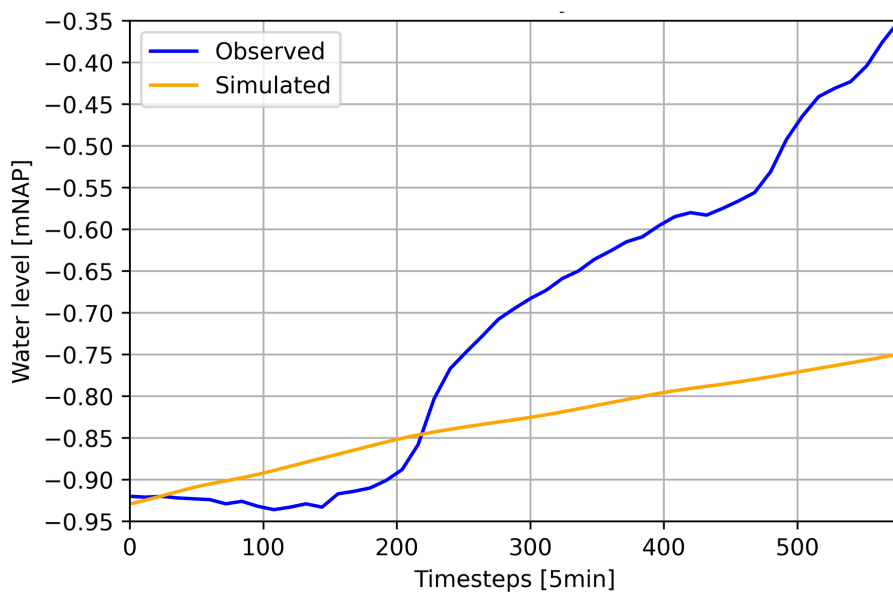
Figure 29: Groundwater levels at the 1e van Leyden Gaelstraat during 12 and 13 October 2023.
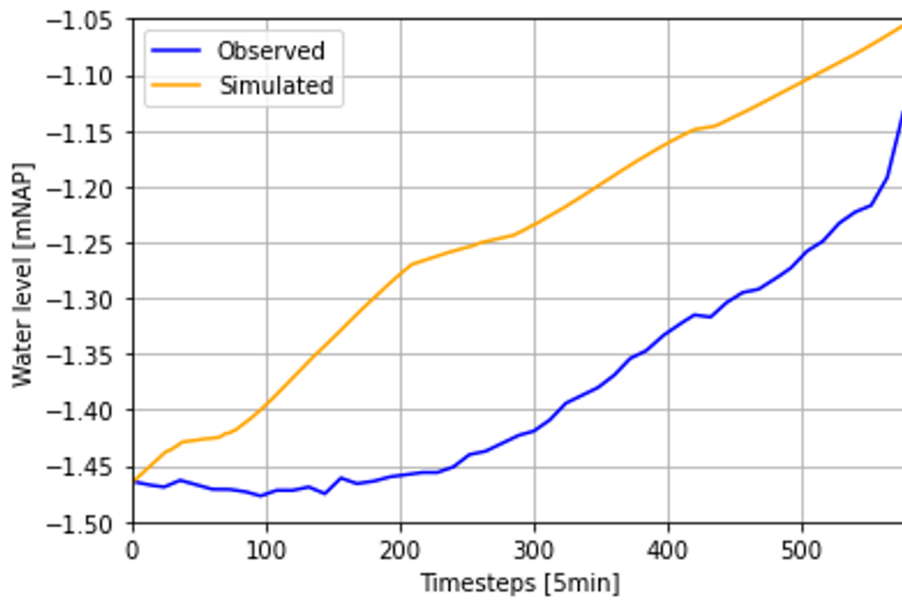
Figure 30: Groundwater levels at the Hogelaan during 12 and 13 October 2023.
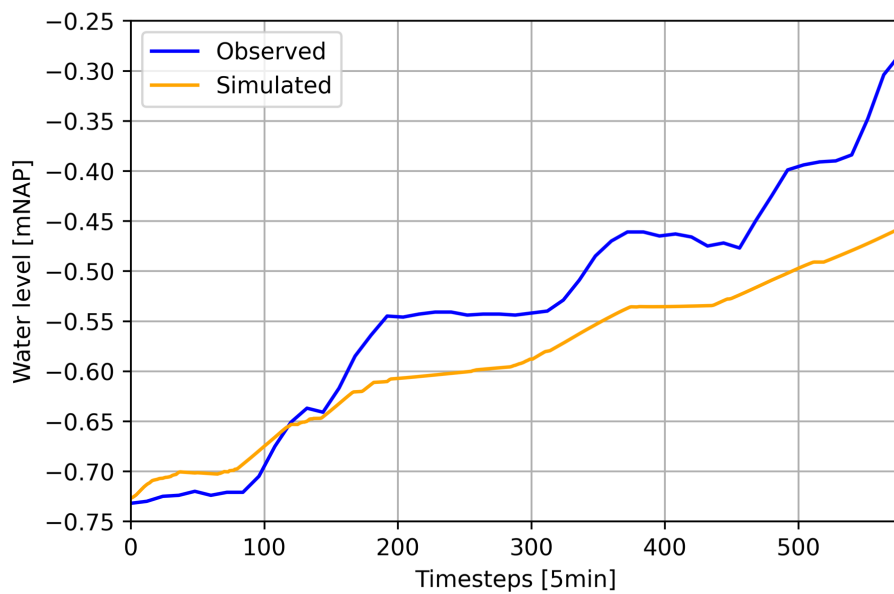
Figure 31: Groundwater levels at the 2e Maasbosstraat during 12 and 13 October 2023.
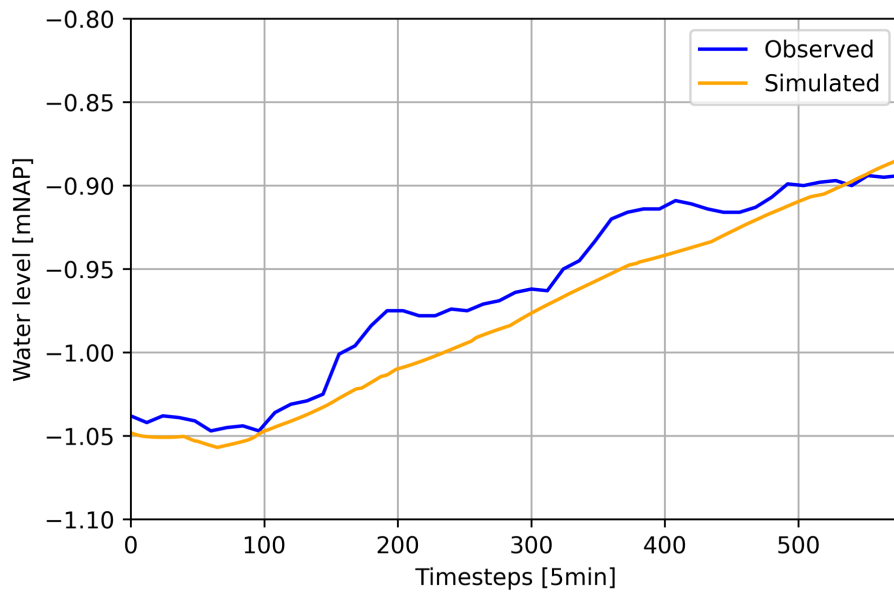
Figure 32: Groundwater levels at the Nieuwstraat during 12 and 13 October 2023.
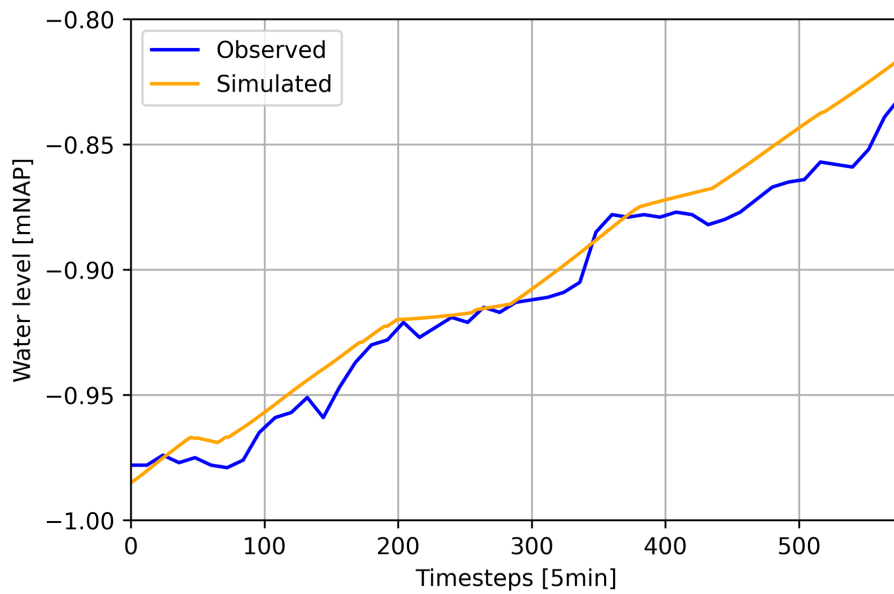
Figure 33: Groundwater levels at the Schiedamseweg during 12 and 13 October 2023.
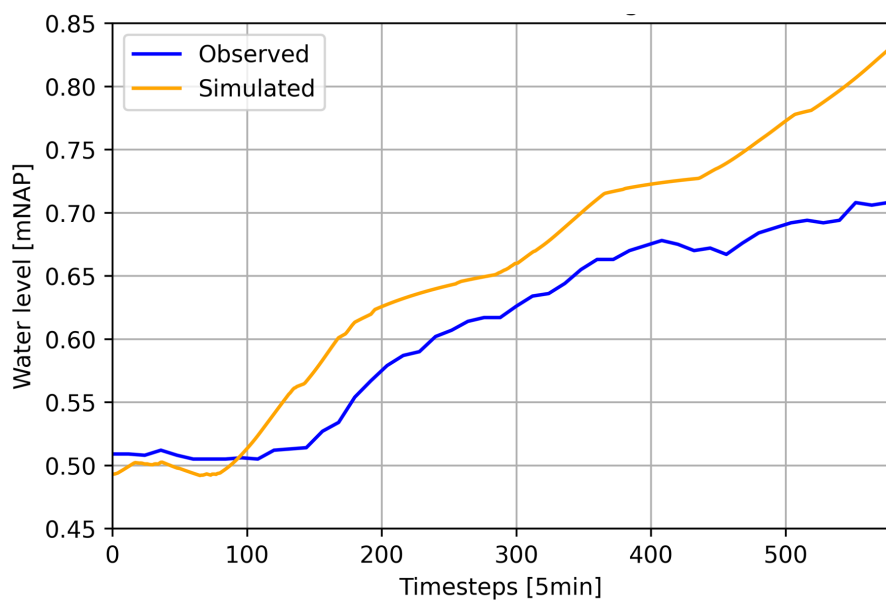
Figure 34: Groundwater levels at the Van Arenbergstraat during 12 and 13 October 2023.

C   Model settings

Physical settings
Use advection 1D: Momentum conservative scheme
Use advection 2D: off

Numerical settings
Pump implicit ratio: 0.00
CFL strictness factor 1D: 1.00
CFL strictness factor 2D: 1.00
Convergence EPS: 0.00001
Convergence CG: 0.000000001
Flow direction threshold: 0.000001
General numerical threshold: 0.00000001
Use of CG: 20
Use nested Newton: on
Limiter water level gradient 1D: 1
Limiter water level gradient 2D: 1
Max non linear Newton iterations: 20
Max degree Gauss Seidel: 7
Min friction velocity: 0.050
Min surface area: 0.00000001
Preismann slot: 0.00
Limiter slope thin water layer: 0.01
Flooding threshold: 0.0001
Friction shallow water depth correction: off
Time integration method: Euler implicit
Limiter slope cross sectional area 2D: off
Limiter slope friction 2D: off
Use preconditioner CG: standard

Timestep settings
Time step: 5.00
Output time step: 300.00
Min time step: 0.01
Max time step: 30.00
Use time step stretch: off